



FLOOD RISK MAPPING USING HEC-RAS MODEL: CASE STUDY ON WAJA
WATERSHED IN RIFT VALLEY BASIN CENTRAL ETHIOPIA REGION, ETHIOPIA.

M.Sc. THESIS

ATEREFE TAMIRAT DEBOCH

HAWASSA UNIVERSITY HAWASSA, ETHIOPIA

NOVEMBER, 2024

FLOOD RISK MAPPING USING HEC-RAS MODEL: CASE STUDY ON WAJA
WATERSHED IN RIFT VALLEY BASIN CENTRAL ETHIOPIA REGION, ETHIOPIA

ATEREFE TAMIRAT DEBOCH

A THESIS SUBMITTED TO THE
FACULTY OF BIO-SYSTEMS AND WATER RESOURCE ENGINEERING DEPARTMENT
OF HYDRAULIC AND WATER RESOURCE ENGINEERING HAWASSA UNIVERSITY
INSTITUTE OF TECHNOLOGY, SCHOOL OF GRADUATE STUDIES
HAWASSA UNIVERSITY
HAWASSA, ETHIOPIA
IN PARTIAL FULFILLMENT OF THE REQUIREMENTS FOR
THE DEGREE OF MASTER OF SCIENCE IN HYDRAULIC ENGINEERING

JANUARY, 2024

SCHOOL OF GRADUATE STUDIES
HAWASSA UNIVERSITY ADVISORS' APPROVAL SHEET

This is to certify that the thesis entitled “**FLOOD RISK MAPPING USING HEC-RAS MODEL: CASE STUDY ON WAJA WATERSHED IN RIFT VALLEY BASIN CER, ETHIOPIA.**” submitted in partial fulfillment of the requirements for the degree of **Master's** with specialization in **Hydraulic Engineering**, the Graduate Program of the **Department of Hydraulic and Water Resource Engineering**, and has been carried out by **Aterefe Tamirat Deboch** ID.No.**GpHyW/0003/14**, under our supervision. Therefore we recommend that the student has fulfilled the requirements and hence hereby can submit the thesis to the department.

Dr. Abebe Tadesse (PhD)

Name of major advisor

Signature

Date

Petros Yohannes (M.Sc)

Name of co-advisor

Signature

Date

SCHOOL OF GRADUATE STUDIES

HAWASSA UNIVERSITY EXAMINERS' APPROVAL SHEET

We, the undersigned, members of the Board of Examiners of the final open defense by Aterefe Tamirat have read and evaluated his thesis entitled “FLOOD RISK MAPPING BY USING HEC-RAS MODELING: CASE STUDY ON WAJA WATERSHED IN RIFT VALLEY BASIN SNNPR, ETHIOPIA.”, and examined the candidate. This is, therefore, to certify that the Thesis has been accepted in partial fulfillment of the requirements for the degree of Master of Science in Hydraulic Engineering.

Aterefe Tamirat

Student

Signature

Date

Abebe Tadesse (PhD)

Advisor

Signature

Date

Alemu Osore (PhD)

External examiner

Signature

Dec 27/2024

Date

Tewodros Meless (PhD)

Internal Examiner-1

Signature

January 19/2025

Date

Internal Examiner-II

Signature

Date

SGS Approval

Signature

Date

DECLARATION

I hereby declare that this research work titled “**Flood Risk Mapping Using HEC-RAS Model: Case Study on Waja Watershed in Rift Valley Basin Central Ethiopia Regional State, Ethiopia.**” is my original work and has not been presented for a degree in any other university, and all sources of material used for this Thesis have been duly acknowledged.

Name: _____

Signature: _____

Date: _____

DEDICATION

This Thesis is dedicated to the memory of my Father Tamirat Deboch. Gashe, you are the main reason for being what I am.

ACKNOWLEDGMENTS

First of all, I would like to thank the almighty God for his endless and invaluable help to be a person of this stage and being able to complete this Master's program. Next, my deepest appreciation and respect full thanks will go to my advisor **Dr. Abebe Tadesse**, for his constructive guidance, innovative suggestions, and the leading role which contributed to the successes of this thesis research.

I am highly indebted my Co- advisor **Mr. Peteros Yohannes**, for all the supports and guidance he has extended to me during my study. I do not think that I would have reached this stage without your genuine advice. He is very supportive, willing and generally great.

I would like to appreciate the Ministry of Water, Irrigation, and Energy particularly Hydrology and GIS department and that provided me with the data and information needed for this work.

I take this opportunity to thank all my friends, who helped me in one way or another, in carrying out my research through remarkable encouragement, advice, material support, and collaboration in every aspect Specially SDCSE GIS and hydrology team greatly appreciated.

Finally, my Special acknowledgment goes to my **Wife Alem Regassa** for her advice, helping in various ways, and encouraging me.

TABLE OF CONTENTS

.....	iii
DECLARATION.....	iv
DEDICATION.....	v
ACKNOWLEDGMENTS.....	vi
LIST OF TABLES	x
LIST OF FIGURES	xi
LIST OF ABBREVIATIONS.....	xii
ABSTRACT	xiii
1. INTRODUCTION	1
1.1. Background.....	1
1.2. Statement of Problem	2
1.3. Objective of the Study	4
1.3.1. General Objectives	4
1.3.2. Specific Objectives.....	4
1.4. Research Questions	4
1.5. Scope of the Study.....	4
1.6. Significance of the Study	5
2. LITERATURE REVIEW.....	6
2.1. Flood characterization.....	6
2.2. Types of floods.....	7
2.3. General overview of flood	8
2.4. Causes and Consequences of Flooding.....	10
2.5. Rainfall-Runoff model Selection	10
2.5.1. Hydrologic Engineering Center's Hydrologic Modeling System (HEC-HMS)	11
2.5.2. Soil and Water Assessment Tool (SWAT)	13
2.6. Calibration and validation of hydrological models.....	13
2.7. Hydrodynamic models.....	14
2.7.1. Model selection criteria.....	15
2.8. Flood hazard mapping	17
2.9. Flood Vulnerability.....	18

2.10.	Flood risk mapping	19
2.11.	Flood Mitigation Measure	20
2.12.	Previous studies.....	21
3.	MATERIALS AND METHODS.....	23
3.1.	Description of the area	23
3.1.1.	Locations.....	23
3.1.2.	Climate.....	24
3.1.3.	Soils.....	24
3.1.4.	Land Use Land Cover of an Area.....	25
3.1.5.	Topography of area	26
3.1.6.	Slope of an area	27
3.1.7.	Hydrologic characteristics of Waja watershed	28
3.2.	Materials.....	29
3.3.	Methods.....	30
3.3.1.	Data collection.....	30
3.4.	Data Analysis.....	31
3.4.1.	Tests on hydrologic data.....	31
3.4.2.	Consistency checks and Adjustment of Rainfall Data.....	34
3.4.3.	Goodness of fit test	35
3.4.4.	Determination of Areal Rainfall.....	36
3.5.	Hydrological modeling using HEC-HMS model.....	38
3.5.1.	Basin characteristics	42
3.5.2.	Calibration and Validation of the Model Parameters.....	42
3.5.3.	Model Performance Evaluation Criteria	43
3.5.4.	Flood Frequency Analysis	44
3.6.	Hydraulic Modeling Using HEC RAS model.....	45
3.6.1.	Mesh Generation.....	46
3.6.2.	Manning's roughness coefficient.....	46
3.6.3.	External 2D Flow Area Boundary conditions unsteady simulation	47
3.6.4.	Post Processor	48
3.6.5.	2D energy equation (Mass Conservation)	49
3.7.	Flood Hazard map.....	49

3.8.	Flood vulnerability map	50
3.9.	Flood Risk Analysis.....	51
4.	RESULTS AND DISCUSSION	52
4.1.	HEC-HMS Hydrologic model simulation	52
4.1.1.	Model Calibration	52
4.1.2.	Model Validation	54
4.1.3.	Peak flood hydrographs.....	55
4.2.	Flood inundation boundaries	56
4.3.	Flood depth.....	58
4.4.	Flood Velocity	59
4.5.	Flood hazard map	60
4.6.	Flood Vulnerability Map	63
4.7.	Flood Risk Map	65
5.	CONCLUSION AND RECOMMENDATION	67
5.1.	Conclusion	67
5.2.	Recommendation	68
6.	REFERENCES.....	70
7.	ANNEXES.....	79

LIST OF TABLES

Table 3.1: Rainfall data stations availability and Location30

Table 3.2: River Flow stations data availability and Location.....31

Table 3.3: D-index values of different distributions36

Table 3.4: Basin parameters of Waja watershed42

Table 4.1: model performance measures during the calibration53

Table 4.2: model performance measures during the validation54

Table 4.3: Flood areal coverage’s with corresponding flood frequency57

Table 4.4:Flood Depth and Velocity Severity Grid Categories source: FEMA (2018)61

Table 4.5: Flood hazard coverage of Waja River.....63

Table 4.6: Flood Vulnerability coverage of Waja River64

Table 4.7: Flood Risk coverage of Waja River66

LIST OF FIGURES

Figure 3.1: Location map of Waja River catchment.....	23
Figure 3.2 : Soil map of the Area	25
Figure 3.3 : Land use Land Cover map of the Area	26
Figure 3.4 : DEM of the study area	27
Figure 3.5 : Waja Watershed Slope map.....	28
Figure 3.6: Double mass curve.....	35
Figure 3.7: Area coverage of Rainfall Stations	37
Figure 3.8: Waja river watershed in HEC HMS model	38
Figure 3.9: Frequency storm depth.....	45
Figure 3.10: Mesh generation within 2D Area.....	46
Figure 4.1: Simulated and observed flows during calibration.....	53
Figure 4.2: Simulated and observed flows during Validation.....	55
Figure 4.3: Flood hydrograph for different return period	56
Figure 4.4: River inundation for 10 years storm frequency	57
Figure 4.5: Waja river flood depths.....	58
Figure 4.6: Flood velocity of Waja River for different storm frequency	60
Figure 4.7: Flood hazard classes of 100 year flood.....	62
Figure 4.8: Flood vulnerability map of Waja River floodplain.....	64
Figure 4.9: Flood risk map of Waja River floodplain	66

LIST OF ABBREVIATIONS

AHP	Analytical Hierarchy Process
AIRM	Aggregated Indices Randomization Method
ANP	Analytic Network Process
BWM	Best Worst Method
CBA	Choosing By Advantages
CER	Central Ethiopia Region
COMET	Characteristic Objects Method
CR	Consistency Ratio
DEM	Digital Elevation Model
FAO	Food and Agriculture Organization
GIS	Geographic Information System
HEC-HMS	Hydrologic Modeling System
HEC-RAS	Hydrological Engineering Centre River Analysis System
MCE	Multi Criteria Evaluation
Mha	Million Hectares
MoA	Ministry of Agriculture
MoWE	Ministry of Water and Energy
MoWR	Ministry of Water Resources
NGA	National Geospatial Intelligence Agency
NMSA	National Meteorological Services Agency
NRSs	National Regional States
OCHA	United Nations Office for the Coordination of Human Affairs
R.I	Random index
SNNP	Southern nation's nationalities and people
TIN	Triangular Irregular Network
UNESCO	United Nations Educational, Scientific and Cultural Organization
USGS	United States Geological Survey

ABSTRACT

Flood is among the most devastating natural disasters worldwide, significantly affecting human lives and property. The current study conducted on the Waja River floodplain aimed to model and maps the flood inundation, flood hazard, flood vulnerability, and flood risk associated with flooding in the area. To achieve this objective, various data sources were utilized, including meteorological, hydrologic, and topographic data collected from different organizations. The study employed several tools and materials, including the HEC HMS and HEC-RAS models, GIS software, GPS devices, and metering tape. The HEC HMS model was used to analyze flood hazard and risk by developing inflow design floods for different return periods. The model was calibrated and validated using actual stream flow data. During model calibration the NSE value was 0.75, Percent Bias (PBIAS) was 2.02, coefficient of determination (R^2) was 0.78, and Relative Mean Square Error (RMSE) was 2.03. During the validation period, the model achieved an R^2 of 0.77, NSE of 0.76, PBIAS of 1.64, and RMSE of 1.3. After calibration and validation, the annual maximum precipitation from rainfall data was extracted to develop frequency storms for different return periods. These storms were then used as input for the HEC HMS model to generate flood hydrographs. The HEC-RAS model, combined with the flood hydrographs, was used to produce flood inundation maps, which were visualized in ARC-GIS software for detailed analysis. The results of the study indicated that for return periods of 10, 25, 50, and 100 years, the areas inundated by floods were 3030 ha, 3364 ha, 3520 ha, and 3683 ha, respectively. Additionally, the maximum flood depths were found to be 6.3m, 9.2m, 12.6m, and 14.45m for the respective return periods. The maximum flood velocities were 3.8 m/s, 4.7 m/s, 5.5 m/s, and 6.8 m/s for the same return periods. Flood hazard maps were derived from the depth, velocity, and duration of floodwaters, revealing that 35% of the flooded area was categorized as having very high and high hazard, while approximately 65% was classified as medium and low hazard. The flood vulnerability map classified approximately 17% of the flooded area as having high and very high vulnerability. About 18% of the flooded area fell into the moderate vulnerability class. The majority of the flooded area, approximately 65%, had low and very low vulnerability. By combining the flood hazard and vulnerability information, the study developed a flood risk map. The results showed that 24% of the area fell into the high and very high-risk categories.

Key Word: Flood risk mapping, HEC-HMS, HEC-RAS, Arc GIS, Rainfall-runoff modeling

1. INTRODUCTION

1.1. Background

Among the natural hazards capable of causing a disaster, the flood is the most hazardous, frequent, and widespread catastrophic events throughout the world today. Between 2000 and 2008, floods were affected the largest number of people worldwide, averaging 99 million people per year. This makes flooding an important subject of study, particularly in the less developed countries like Africa and the others. According to the related Programs on Flood Management, flood impacts tend to be very dangerous in African towns where improper land use planning and management for urbanization takes place. (Abu, 2020)

Flood can be defined as any relatively high water flow that exceeds a natural or man-made bank in any part of a river or stream. People can be swept away in a short time and property can be severely damaged by floods. When a riverbank is submerged, water overflows the floodplain and often becomes a hazard. Flooding is the most common environmental hazard due to the wide geographical distribution of river valleys and coastal areas. Attracting people to these areas for settlement and farming makes them a serious obstacle to social progress in both developing and developed countries (Jayaseelan, 2001).

Most countries in the world experience floods and flooding. The risk of flooding is enormous. These natural hazards cause damage to life, property, and ecosystems. Flooding is one of the major natural hazards in Ethiopia due to a national topography of mountainous highlands and lowland plains with natural drainage systems formed by major river basins. Flash floods are a common flooding problem caused by high runoff from the surrounding mountains (Adhanom, 2019) .

Flood impact mitigation requires information about flood characteristics and how those characteristics propagate. Information about flood properties could be obtained from hydrodynamic models. Hydrodynamic models can simulate flood extents, depths, levels, velocities, and times over a distributed model domain and over the time dimension. Such flood models solve relevant flow equations based on the laws of conservation of mass, energy, and momentum.

Structural and non-structural measures are being taken worldwide to reduce flood damage. However, it is time-consuming and costly to thoroughly construct flood defenses to reduce the risk of flood damage. Flood risk maps are essential to achieve this goal, helping local residents to be aware of the vulnerability of the area they live in, the important role they play in disaster prevention measures, and proper evacuation in the event of flooding.

The Waja watershed is located in the lower basin of the Ziway Lakes in the Rift Valley lake basin system and is territorial in the Gurage and Silte Zone, CER, Ethiopia. The river often causes flooding in the upstream highlands around the Zebider Mountains in the summer season after heavy rains. Tributaries such as Angelo, Labogarobe, Labo, Murtute, Garore, Tineshu Abay and Irinzaf (Butajira), Overflow into the Waja River in a short time, causing flooding in the low-lying alluvial plains along the course of the river around the Goflala Kebele. Heavy rains in the upstream catchments cause large inflows into Ziway Lake.

Therefore, developing a rainfall-runoff model and a mapping of flood risk is an important task. Consideration of both rainfall-runoff modeling and flood risk mapping for the downstream Waja River serves to minimize its impact on community life and property by knowing the path of the problem.

1.2. Statement of Problem

Flooding is one of the most devastating natural disasters globally, and Ethiopia is no exception specifically the Silte Zone, particularly in the Waja watershed, the frequency of flood events has increased significantly over the years. The Silte Zone's unique geographic features, including its highland mountains and lowland plains, contribute to its susceptibility to flooding. The area suffers from severe land degradation, which aggravate soil erosion and reduces the land's ability to absorb rainfall. Consequently, heavy rains lead to excessive runoff, overwhelming natural drainage systems and causing widespread flooding. This environmental degradation not only heightens flood risks but also compromises the region's ecological balance. The Silte Zone is known for its agricultural productivity, which is vital for the food security of Ethiopia. However, recurrent flooding threatens this productivity by inundating vast areas of farmland, displacing crops, and damaging agricultural infrastructure. The loss of crops directly impacts the livelihoods of

farmers and their families, leading to food shortages and increased poverty levels in the community.

Upstream catchment of the Waja is characterized by high upland erosion by different small Tributaries (i.e. Angelo, Labogarobe, Labo, Murtute, Garore Tineshu Abay and Irinzaf (Butajira). Most of these tributaries flowing to common reach at Waja Watershed particularly at Goflala Kebele whose elevation is low; have been caused flooding for Fourteen Kebeles including Guraghe Zone. Historical flood events were recorded on Goflala that displaced a number of inhabitants from the area. According to the report from the Agriculture Department of Silte Zone, the flood disaster currently affecting six Kebeles across two districts has resulted in the displacement of over 1,000 households and left more than 5,000 residents homeless. This significant increase in the number of evacuees highlights the urgent need for effective disaster management and response strategies. The flooding has severely impacted local agriculture, inundating more than 1,400 crop fields and displacing over 5,000 livestock. This situation not only threatens food security but also jeopardizes the livelihoods of many families in the region, emphasizing the necessity for targeted agricultural support and recovery plans.

The Silte Zone Disaster Risk Management Office has reported that this disaster has been ongoing since May, and support has been provided for those affected. Although the Silte Zone administration has allocated over 1.7 million birr in assistance, stakeholders including displaced residents have indicated that this support is insufficient to meet their immediate needs. The gap between the scale of the disaster and the level of assistance available calls for a comprehensive evaluation of resource allocation and support mechanisms were not balanced.

Meteorological forecasts suggest that worsening winter conditions may exacerbate the ongoing disaster, indicating a potential increase in both the frequency and severity of flooding events. This raises concerns about the long-term resilience of affected communities and underscores the need for proactive measures to mitigate future risks. Despite the involvement of federal, regional, and zonal leaders in assessing the situation, there is a pressing need for improved coordination among various stakeholders to ensure that relief efforts are efficient, comprehensive, and address the specific needs of the displaced populations.

This situation necessitates urgent intervention to protect agricultural activities and ensure the sustainability of local economies. Current methodologies for assessing flood risk in the Silte Zone primarily rely on flood extent maps, which do not adequately capture the complexity of flood dynamics. Traditional assessments often overlook critical factors such as flood depth, velocity, and duration, which are essential for understanding the true risk faced by communities. With advancements in hydrodynamic modeling techniques, it is now possible to create more accurate flood hazard and risk maps. These models can inform local authorities and stakeholders about potential flood impacts, allowing for more effective preparedness and response strategies.

1.3.Objective of the Study

1.3.1. General Objectives

The General objective of this study was to develop the flood hazard and risk map of Waja river water using HEC RAS model

1.3.2. Specific Objectives

The specific objectives of this study are:

- To estimate peak Floods of the study area for different return periods.
- To develop a flood Inundation and hazard map of the study area.
- To develop a flood risk map for the study area.

1.4.Research Questions

- ❖ What are the estimated peak flood levels for the study area across different return periods?
- ❖ How can a flood inundation and hazard map for the study area is developed to identify areas at risk?
- ❖ What is the flood risk level of a study area?

1.5.Scope of the Study

The studies were focused on the Silte Zone, specifically within the Waja watershed. This area has been significantly affected by recurrent flooding, impacting local communities, agriculture, and infrastructure. The study were involved the development of a flood risk map using hydrodynamic modeling techniques, such as HEC-RAS, to assess flood depth, speed, and duration. It was also identify flood buffer zones critical for future planning and investment in infrastructure projects.

1.6. Significance of the Study

This study aims to improve disaster management strategies in the Silte Zone, where flooding has become a recurring event. By assessing the current situation and identifying gaps in response efforts, the study can inform local authorities and stakeholders on how to enhance preparedness and develop more effective response plans for future flood events. One of the key contributions of this study is the development of a flood risk map that offers valuable information to area officials, emergency managers, and local residents. This map was serving as a critical tool for planning emergency responses, helping to identify high-risk areas and prioritize resource allocation during flood events. The studies were identifying flood buffer zones that should be considered when planning and investing in significant projects in the area. Recognizing these zones is crucial for sustainable development, as it helps mitigate risks associated with flooding while ensuring that infrastructure projects do not exacerbate existing vulnerabilities.

2. LITERATURE REVIEW

2.1.Flood characterization

Flood is defined as the inundation of land by the rise and overflow of a body of water, which may result in some property damage, occasionally fatalities, and injuries. Water resources experts usually associate flooding with flows that are close to their yearly peaks in volume. The most harmful and severe natural disasters are floods. In addition to the loss of human and animal life, they result in extensive damage to farmland, homes, and public utilities and cost billions of dollars annually. (Roy, S.K. and Sarker, S.C., 2016)

Flood is among the most common and destructive natural hazards known for their extensive damage to infrastructure, public and private services, the Environment, and the economy and destruction to a residential area. Floods stand out to be the most frequent and devastating natural disaster around the world (Sinha, 2005), affecting millions of people every year.

According to (Subramanya K. , 2009), Flood is an unusually high level in a river, normally the stage at which the river overflows its bank and inundates the plain area. The damage cause by flood in terms of loss of property and economic loss due to disruption of economic activity are all too well known. Wide range of cores of rupees is spent every year in flood control and flood forecasting.

Flooding is a natural occurrence that takes place frequently and in many different places. Overflow from the sea and from rivers is perhaps best recognized, but sewage overflow, overland flow, and ground water flooding can also be brought on by prolonged, strong, and localized rainfall. Flooding has a big influence on human activity and can endanger lives, property, and the environment. Housing, transportation, and utility infrastructure, as well as business, industrial, and agricultural operations, can all be considered assets. As a result of climate change, flooding is predicted to become more frequent and severe. By accelerating and enhancing surface water runoff, changing water courses, and reducing flood plain storage, development can exacerbate the issue of floods. (Khan and Rahman, 2015)

Flooding in Ethiopia often happens during the three months of the rainy season and is only seen in regions with a low and flat topography. Highland rainfall is typically what

causes floods downstream and calamity for communities near any stretch of river courses (Abu, 2020).

2.2. Types of floods

Flood types may generally be classified by identifying the primary distinctions between each type of flood. This is done by taking into account variables like the impacted area's size and the driving precipitation event's duration. This leads to the two primary classifications of extensive long-lasting floods and small abrupt floods, which are useful in defining the spatial and temporal scale of flood events. (Bronstert, 2003)

Most common flood types reported in literature are briefly described and include the following;

Coastal floods: this is a type of floods that occur along the coasts of the seas and big lakes. The triggering factor for this type of floods are wind storms such as cyclones and low atmospheric pressure that eventually result to the set-up of water levels on the coast. It is mentioned that when this set-up of water levels coincides with astronomical high tide at the coast, coastal floods can lead to high water levels and thus flooding of the coastal area (Jonkman, 2005)

Flash floods: is a particular kind of flooding that happens quickly following a precipitation event, usually within less than six hours. It frequently occurs in locations near rivers or lakes and is brought on by high or excessive rainfall, though it can also occur in areas without any nearby bodies of water. (Camp J. , 2022) Steep slopes, impermeable ground surfaces, and soils with low permeability are other characteristics that have been linked to this type of flooding (Camp J. , 2022). The prediction and cautioning becomes troublesome in light of the abrupt event of flash floods by leaving very brief timeframe. Moreover the high increasing rate and flow velocity of flash floods likewise make them more dangerous to human lives than river floods (Camp J. , 2022). Property damage and Death caused by flash flood are more articulated when contrasted with other type of floods (Jonkman, 2005).

River floods: refers to a flood type caused as a result of flooding of the river outside its regular boundaries. They can likewise be related by a break of barriers or dams close to the river. As per (Jonkman, 2005), river floods can be caused by various sources

including high precipitation levels, melting snow and blockage of the flow. Unlike flash floods, river floods can be predicted in some period in advance (Jonkman, 2005)

2.3. General overview of flood

Floods are among the greatest threats to social security and the sustainable development of society (Dottori et al., 2018), (Jahandideh-Tehrani et al., 2021) and; (Mishra et al., 2022) and are among the most traumatic natural hazards in many parts of the world. Heavy rainfall, rapid snowmelt, storm surges from tropical cyclones, or tsunamis is the hydro meteorological causes of floods (Mishra et al., 2022).

Globally, flooding is a leading cause of losses from natural disasters and responsible for a greater number of damages than most other types of elemental threats (Debarati, 2006). According to (Debarati, 2006), South-East Asia, which is part of the most flood hit continent in the world, topped the list of disaster impacts over the first six months of 2006, with 85% of global deaths from natural disasters over this period. These were a total of 113 floods during this period, globally representing all-time high of 65% of all natural disasters.

According to (Central Water Commission, 2020), Between 1953 and 2019, floods in India cost INR 62.08 billion annually on average due to damage to crops, homes, and public services, as well as the loss of 1674 lives. The hydrological cycle was accelerated by changes in land use and human warming, which in turn enhanced the frequency, amplitude, duration, and intensity of intense rains. (Singh et al., 2020); (Mishra et al., 2022). In addition, urban centers situated on the coast and riverbanks are at high risk of flooding due to sea level rise, poor natural drainage, rapid urbanization, and encroachment in the floodplain (Sherly et al., 2015),

According to (SALHA|N, JUN RENTSCHLER & MELDA, 2020), Some 2.2 billion people, or 29% of the world population, live in locations that are estimated to experience some level of inundation during a 1-in-100-year flood event. Such an event has a 1% chance of occurring in any given year, which translates to a 10% probability in a decade, or 50% in a lifetime (68 years). About 1.47 billion people, or 19% of the world population, are directly exposed to inundation depths of over 0.15 meters. Furthermore, for over half of this exposed population, flooding could be even higher reaching life-threatening levels, especially for children and the disabled. The most devastating long-term consequences of floods are often experienced by the poorest households those who

have next to no savings and limited access to support systems. By considering the dimension of poverty, it is possible identify where floods would cause prolonged adverse impacts on livelihoods and well-being. By this measure, countries in sub-Saharan Africa face the greatest threat: We estimate that of the 171 million flood-exposed people in this region, at least 71 million people live in extreme poverty (i.e. living on less than \$1.90 a day). Globally, 587 million poor people are exposed to flood risk, 132 million of which live in extreme poverty.

In Ethiopia, flood usually takes place at the peak of the rainy season (July and August) in most flood-prone areas. In East shoe Oromia region flooding often happens during July and August. In study area Unseasonal and above-normal rainfall during September to October could also cause flooding in areas along Awash Rivers. (Mokonen, 2021).

According to (Belina, 2020), Floodplains, which are typically found along rivers at their downstream portions, are a common flood hazard. One of the five major basins that have encountered extensive floodplains along its path is the Awash River Basin. Once a year, during the summer wet season, known flood occurrences are known to occur at its middle and lower catchments. The primary tributaries of the Awash River, the Mille and Logiya, overflow in the lower catchments, posing a risk to settlement and agriculture. The Kesseme and Kebena tributaries of the Awash River also contribute significantly to flooding in the middle watershed. Additionally, there are additional basins where there are significant flood dangers for both property and habitation.

According to (Alemu, 2015), During flood occurrence in Dire Dawa during in August 1981 80 people were killed , and the other unpredicted flood that occurred on August 6, 2006 flooding was worst of all flooding event in Dire Dawa that killed 256 people from which 244 were missed and 15,000 people were displaced. In 2006 a total of 524,400 people were vulnerable to flood disaster throughout the country during the rainy season of Ethiopia. Out of this population, 199,900 people are actually affected by flood disaster in various regions of the country. The socio economic sector was badly impacted by the 2006 floods in Dire Dawa, which resulted in 256 fatalities, 244 unaccounted for, more than 9956 displaced people, and estimated property damage of 17,146,493 ET. Birr for 882 small-scale traders and 123 licensed traders. Due to the costs of restoration and construction, it also had a significant influence on the city's economy. While the capital expenditure remained constant or even reduced, the city's ongoing expenses for

renovation and reconstruction grew by 43%. Flood-related direct and indirect losses to the city's agricultural, commercial, and infrastructural sectors were around 97,368,634.36 ET Birr. The implementation of land-use policy is crucial for the future.

2.4. Causes and Consequences of Flooding

According to (Tekle, 2020), flooding is caused by many factors, such as structures that held back the water. In another way, flooding can be exacerbated by increased amounts of impervious surface or hard ground cover that does not let water through, as well as other natural hazards such as wildfires that reduce supplies or the amount of vegetation cover that can absorb rain.

(Tekle, 2020) Indicate that flooding can occur due to meteorological, partly meteorological, or other causes that can aggravate the occurrence of flooding. Meteorological causes are snowmelt, rain and a combination of rain and ice melt. Coastal storm surges and estuary interactions between current flow and tidal conditions bring about partly meteorological causes. The remaining causes of flooding can be attributed to other natural hazards such as earthquakes, landslides, tsunamis, and hurricanes or man-made (technological) hazards such as dam breaches, levees, dikes, weirs, and terraces. The cause of flooding can be described in terms of the water source, the geography of the receiving watercourse, the cause, and the speed of occurrence. Water source-related flooding can originate from the ocean (coastal floods), rivers (river floods), underground (groundwater floods), and rain (pluvial floods). These major flood types are each described in terms of their geography, cause, and speed of onset.

According to (Cançado, 2010) quoted in (Tekle, 2020), floods have both direct and indirect consequences. Furthermore, as noted (Zein, 2010), direct losses from flooding include deaths, injuries, homelessness, the collapse of buildings and infrastructure, sedimentation, pollution, and so on. Indirect losses include disease, psychological impact, short- and long-term economic loss, and so on.

2.5. Rainfall-Runoff model Selection

The relationship between the catchment's surface runoff production and the precipitation the catchment receives is demonstrated through rain-runoff modeling. The target catchment area's surface runoff is estimated by the model as a function of precipitation in the canal or river system. Rain-runoff modeling aids in the visualization of the changes

that past surfaces, vegetation, and climatic events have brought about in the water system. (Namara, 2020).

According to (Xiang, 2020), the mechanism for making decisions regarding flood protection has benefited from flood forecasting. The confidence level and lead time of flood predictions are used to guide decision-making. Estimating the flood volume is essential to a quantitative analysis. The most crucial factor in designing waterworks for flood mitigation strategies is this one. The model is used in conjunction with other approaches to examine the hydrograph's fluctuation throughout a range of return intervals. The runoff and subsurface runoff that contribute to stream flow are calculated using a conceptual model in the rainfall-runoff model, which interprets the hydrological processes (Manfreda, 2008).

According to (Namara, 2020), the models are used as tools for a variety of activities, including forecasting floods, modeling the flood event, and observing water levels in various water scenarios. There are deterministic and probabilistic hydrological models. Results from the probabilistic models exhibit some degree of randomness, but those from the deterministic models do not.

2.5.1. Hydrologic Engineering Center's Hydrologic Modeling System (HEC-HMS)

The conceptual representation of watershed activity by HEC-HMS is as various runoff process components. Its specification is based on the information requirements of the hydrological research and contains an accurate depiction of the hydrological system. Accurately forecasting catchment outflows from upstream sub catchments and flood wave propagation along the drainage network are the primary goals of flood hydraulic modeling and flood inundation mapping. HEC-HMS offers the user freedom by offering a variety of models for each component. For estimating peak discharges and runoff hydrographs for various return periods at various locations of the water shed outlet, the HEC-HMS model is employed. (Yeshmebet Yitbarek Belay, et al, 2022).

According to (Gunathilake, 2019), the key justification for choosing HEC-HMS is that regionalization demands a frugal approach. As a result, using a minimal amount of input data, the model is utilized to simulate runoff for gauged and un gauged catchments. The Swedish Meteorological and Hydrological Institute created the process-based continuous HEC-HMS model in the early 1970s to aid hydropower operations through forecasting.

This concept has been utilized extensively in Finland, Norway, and Sweden, as well as more than 50 other nations. It is less complex approach and effective in simulation. Also, HEC-HMS model has been applied in Ethiopia with success in several studies. It is successfully applied in regionalization for hydrological balance and stream flow prediction in catchments in Upper Blue Nile sub. It also received applications for estimation of stream flow in catchments in Dedessa. (Kemal, Chekole Tamalew & Abdella, 2016) and Upper Tekeze sub basin (Tadesse, 2017), (Akawka & Haile, 2021) also applied HEC-HMS for regionalization of model parameters for predicting stream flows in un-gauged catchments of the Upper Blue Nile basin. Therefore, those studies showed that the HEC-HMS model is capable to predict stream flow in un gauged catchments. HEC-HMS project requires four model data components:

Basin Model: - Basin Model: The basin model serves as a representation of the actual watershed. The user can build a basin model by adding and connecting hydrologic elements. A basin model is made up of numerous hydrologic parts; including reaches that help communicate stream flow, junctions that mix stream flow from areas upstream of the junction, and sub-basins that are used to represent physical watersheds. To compute precipitation loss, excess precipitation translation to direct runoff, base flow estimation, and flood routing, various methodologies are used in the basin model. (Chuanhai Wang et al., 2021)

Meteorological model: - The precipitation and evaporation data necessary to simulate watershed dynamics are stored in the meteorological model manager. The meteorological model manager calculates the input for precipitation for each sub basin. Using both points and gridded precipitation data, this model can simulate both frozen and liquid precipitation as well as evapotranspiration. (Chuanhai Wang et al., 2021)

Control specification: - Time-related information in the simulation, such as the beginning and ending dates and the computing time interval, is referred to as the control specifications. (Mokonen, 2021).

Paired data: - Hydrological models need hydrological recorded data for the paired data component, which is described below. Items of a dependent variable for an independent variable are defined by paired data. The function must increase monotonically, which means that it cannot drop in order for any given example. Different data storage-discharge functions are contained in the paired data component, including elevation storage,

elevation area, elevation discharge, inflow diversion, diameter percentage, cross section, and unit hydrograph curves. The various forms of paired data models are distinct and each uses a different type of data. One entry must be made for each pair of chosen data. Multiple basin models may exchange paired data, which is a component of the project. (Mokonen, 2021).

2.5.2. Soil and Water Assessment Tool (SWAT)

The Soil and Water Assessment Tool (SWAT) is a hydrological model that can be used to simulate the hydrological processes in watersheds, such as rainfall-runoff processes and river flow. The model can be used to estimate the hydropower potential of a river basin by simulating the flow of water within the basin and identifying areas with suitable hydrological conditions for hydropower development. (Sarraf Aloui et al, 2023).

According to past review studies and a large body of literature that currently numbers more than 5000 studies, the Soil and Water Assessment Tool (SWAT) is one of the most widely used eco-hydrological models globally. The assessment of water resource issues, the investigation of hydrological processes, the study of the effects of land use and climate change, and the use of best management practices all involve the use of hydrological and water quality models. (Sarraf Aloui et al, 2023)

As demonstrated by multiple SWAT overview articles for special issues, SWAT has proven to be a reliable and adaptable multidisciplinary modeling tool that may be used to simulate a range of watershed problems. (Sarraf Aloui et al, 2023).

2.6. Calibration and validation of hydrological models

Model calibration is the process of estimating model parameters by comparing model predictions (output) for a given set of assumed conditions with observed data for the same conditions. In model validation, a model is run using input parameters measured or determined during the calibration process. Calibrating on a major flood event does not guarantee that the model will accurately simulate another flood event even when they are of the same magnitude. Keeping this difficulty in mind, multiple peak flow events were selected for calibration. (Hongren Shen, & Bryan A. Tolson, 2022).

The calibration of hydrological models is often complex in regions with scarce data, and generally only uses site-based stream flow data. However, this approach will yield highly generalized values for all model parameters and hydrological processes.

After the model has been calibrated, the evaluation takes place. Hydrological models can be evaluated in many different ways, but typically involve validation of forecast performance under changing conditions, and sensitivity and uncertainty analyses. (Xin Jin and Yanxiang Jin , 2020).

2.7. Hydrodynamic models

Hydrodynamic models are Numerical flood models or computer-based models that use mathematical and computational techniques to simulate the behavior of water during a flood event (Anees et al. 2016). These models typically employ numerical algorithms to solve equations that describe the flow of water in a river or stream, while taking into consideration factors such as rainfall, runoff, channel geometry, and riverbed roughness. Numerical flood models can be used to simulate the effects of various flood scenarios, as well as to assess the efficiency of the proposed flood mitigation measures (Saleh et al. 2013). They are also used to simulate how flood behavior will alter in response to changes in climate, land use, and other factors. Numerical flood models can take several forms, such as one-dimensional models that simulate water flow in a river channel (Pramanik, Panda, and Sen 2010) or two-dimensional models that simulate water flow over a floodplain (Rameshwaran and Shiono 2007).

Hydrodynamic models are widely used tools in detailed flood dynamics simulations and are mostly linked to flood forecasting, mapping (Anees et al. 2016). The critical characteristics of hydrodynamic models that perhaps explain their widespread usage in various applications are the ability to manipulate their inputs to investigate the impacts of changes in the initial conditions, boundary conditions, and topographic changes arising from the change in critical hydrodynamic features such as river streams, culverts, and stream channel volume (Randa et al. 2022). The 1D hydrodynamics are usually computationally efficient since they consider flows in one direction and assume their steady and uniform. However, they have several limitations which include the inability to capture lateral and vertical wave diffusions of the flood waves, considering topography as cross-sections rather than the continuous surface, and thus somehow subjective in factoring in orientation and topographical cross-sections (Horritt and Bates 2002). The 2D hydrodynamics generally can accurately simulate inundation timings and durations and are thus commonly used in different applications. However, they are computationally intensive especially when covering a large study area since they solve the full shallow-water equation (Neelz and Pender 2010). The 3D hydrodynamic models are generally

considered not viable when covering an area of more than 1000 square Kilometers especially when a high-resolution simulation is required. They are computationally intensive and may take prohibitively long and thus not reliable for quick forecasts that give enough lead time for interventions (Beven and Binley 1992). For numerical flood modeling, a number of software packages are available, including:

- HEC-RAS: This software, created by the US Army Corps of Engineers, is used to simulate the hydraulics of river systems in both one and two dimensions (Khattak et al. 2016);
- MIKE FLOOD: This software, which was created by DHI, is utilized for the two- and three-dimensional hydraulic modeling of floodplain and river systems (Tansar, Babur, and Karnchanapaiboon 2020);
- TUFLOW: This software is used for the two-dimensional and three-dimensional hydraulic modeling of floodplain and river systems (Fahad et al. 2020);
- Flood Estimation Handbook (FEH) models: Developed by the United Kingdom Environment Agency, used for rainfall–runoff modeling and flood frequency analysis (Faulkner and Wass 2005);
- Environmental Protection Agency’s Environmental Fluid Dynamics Code (EFDC): This software, developed by the United States Environmental Protection Agency, is used for three-dimensional hydraulic and water quality modeling of surface water systems (Roy et al. 2020)..

It is important to note that the software chosen was determined by the specific needs of the flood study, as well as the availability of data and resources. (Shustikova et al. 2019), (Schubert et al. 2022) and (Chang et al. 2018) compared two 2D numerical models (LISFLOOD-FP and HEC-RAS) used for assessing floodplain flooding, and discovered that although coarser grids perform comparably, higher-resolution grids produce superior outcomes.

2.7.1. Model selection criteria

When selecting both hydrological and hydraulic models for flood modeling, it is important to consider a combination of criteria to ensure the models are suitable for the specific study (Gul, Harmancıoglu, and Gul 2010). Here are some key criteria to consider:

Study Objectives: Clearly define the objectives of the flood modeling study. Determine whether the focus is on rainfall-runoff modeling, floodplain inundation mapping, flood

forecasting, flood risk assessment, or a combination of these objectives. The selected models should be capable of addressing the specific objectives effectively.

Model Capabilities: The hydrological model should capture the rainfall-runoff processes and provide accurate estimates of inflows to the hydraulic model. The hydraulic model should accurately simulate flow dynamics, floodplain inundation, and interactions with hydraulic structures. Consider factors such as model algorithms, available modules, and their suitability for the study area.

Data Requirements: This includes meteorological data, streamflow data, topographic data (e.g., digital elevation models), river network data, boundary conditions, and hydraulic structures. Ensure that the models can utilize the available data sources and formats effectively.

Model Validation and Performance: The validation studies and performance evaluations of both the hydrological and hydraulic models under consideration should be reviewed. The models' testing against real-world flood events should be assessed, and their performance metrics, such as accuracy of flood extent, water depth, and velocity predictions, should be compared. Models with a proven track record of performance in similar study areas should be chosen.

Computational Requirements: The computational requirements of both the hydrological and hydraulic models should be evaluated. Factors such as the models' scalability, processing speed, and memory requirements should be considered. It should be ensured that the available computational resources are sufficient to run both models efficiently, particularly if the study area is large or the models require high-resolution data.

User-friendliness: The ease of use and user-friendliness of both the hydrological and hydraulic models should be considered. The graphical user interfaces (GUIs), availability of documentation and tutorials, and the level of technical expertise required to operate the models should be assessed. User-friendly models can streamline the modeling process and reduce the learning curve for researchers and practitioners.

The availability of technical support: The availability of technical support and updates from the model developers or the modeling community for both the hydrological and hydraulic models should be considered. It should be ensured that the selected models

have active user communities, online forums, and access to technical assistance. Regular updates and bug fixes can enhance the models' performance and address any issues that may arise during the modeling process.

Cost: The cost implications associated with both the hydrological and hydraulic models, including licensing fees, additional modules, and ongoing maintenance costs, should be assessed. The budgetary constraints and available funding for the study should be considered, and the cost-effectiveness of the selected models should be weighed against their capabilities and performance.

2.8.Flood hazard mapping

Flood hazard maps are widely used in flood information reports and requests for updating when changes have occurred in the canals, in the flood plains, and in the upstream areas. These changes include structural and channel or flooding changes in upstream areas. The development of new buildings on the floodplain, obstructions, or other land-use changes can affect water surface elevation, discharge, and flow rates, thereby altering the elevation profile that defines the floodplain

Flood hazard mapping is an essential part of appropriate land use planning in flood-prone areas. It produces easy-to-read, quick-to-access charts and maps that help identify areas at risk of flooding and also helps prioritize mitigation and response actions (G.Venkata Bapalu, 2014)

The flood hazard map is a flood map that shows the flood hazard, i.e. the intensity of flood situations and the associated probability of it being exceeded. A flood hazard map often shows the spatial distribution of water depth and flow velocity for scenarios of synthetic flood plains with a specific return interval. The hazard characteristic of flood risk is related to the hydraulic and hydrological parameters. Geographic information systems (GIS) are often used to create flood hazard maps. They provide an effective way of assembling information from different maps and digital elevation models (Sinha, 2005). GIS can calculate the extent of flooding by comparing local elevations to extreme water levels.

2.9. Flood Vulnerability

Flood vulnerability is one of the significant components in risk management and flood damage assessment. (Nasiri et al., 2016b). Since vulnerability is found to be the main reason for disasters, it seems necessary to develop our perception of vulnerability (Nasiri et al., 2016a). Research with vulnerability subjects involves diverse descriptions for vulnerability; in the United Nations' description vulnerability is a degree of damage to certain objects at flood risk with a specified amount and present in a scale from 0 to 1 (no damage to full damage) (UNU-EHS, 2006). The International Panel on Climate Change (IPCC) described the vulnerability as the incapability degree of managing climate change and sea-level rise impacts (IPCC, 1995). There are several methods developed by Researchers to evaluate flood vulnerability. Nevertheless, flood threat is still very prevalent in spite of increased awareness about the vulnerability (Birkmann, 2007). This matter increases doubt about the effectiveness of vulnerability evaluation methods and their influence on flood mitigation and adaptation (Khan, 2012). Vulnerability measurement is a complex process because it is influenced by several environmental, economic, and social or even political elements in local scale (Nasiri et al., 2016a). In other words vulnerability is affected by numerous factors such as settlements conditions, infrastructure, authority's policy and capacities, social inequities, economic patterns, etc. (Miranda & Ferreira, 2019). So flood vulnerability varies for people in diverse circumstances (Pandey et al., 2010). Human systems are vulnerable to floods due to three vital aspects: Exposure, susceptibility, and resilience. Exposure refers to people and their surroundings and every element present in flood-prone areas being exposed to the flood impacts as a subject to potential losses (UNISDR, 2009). Susceptibility (Tan et al., 2012) states that people, environment, and infrastructure tend to be influenced by a hazard because of the fragility of the community or ecosystem, and (Al, 2004) defines resilience, coping, and adaptation ability of a system in addressing disaster stress. Instance the vulnerability of urban areas is a reflection of the exposure and susceptibility of the city to flood risk and the resilience of that region to cope and recover from the flood effects (Smit, 2006).

Generally, the vulnerability of a system against a certain hazard is not easily assessed. Three routes for the assessment can be distinguished such as economic, social, and cultural.

Thus, vulnerability assessment in flood-prone areas depends on the following factors (Tsakiris, 2007):

- The Exposure of the system (E).
- The initial coping capacity (resources availability) of the system (S).
- The magnitude and intensity of the hazardous event (Q_{max}).
- The social response of the system (early warnings, indigenous experience, public awareness, etc.) (SF).
- The fuzziness of the interrelated sides of vulnerability (coping capacity & exposure) (I).

2.10. Flood risk mapping

Flood risk maps are essential tools for land use planning in flood-prone areas. The basic criteria for mapping are usually chosen according to flood return periods. Sometimes, the expected water depth or dynamic considerations are used instead. These criteria are discussed in mapping examples from several countries. To draw a flood risk map, four phases are usually recognized: hydrologic, geomorphic, hydraulic, and land use. Each of these phases poses different problems and requires relevant methodologies to accomplish them. A flood Risk mapping is the basic tool and starting point of any regional intervention policy for flood control. Flood risk maps can be used for several purposes:

- ✚ they provide the basic initial information for land use planning;
- ✚ they allow correct development for new urban areas;
- ✚ the cost of flooding and risk reduction benefits can be adequately evaluated by using these maps;
- ✚ the feasibility of non-structural flood control measures such as flood proofing can be correctly assessed;
- ✚ they can form the basis for any type of insurance plan;
- ✚ flood risk maps serve as a logical base for investment planning and priority setting, mainly for non-structural measures; and
- ✚ Last but not least, flood risk maps increase public awareness of risk.
- ✚ It's more of a guide to proper resource management than a restrictively-centered mechanism for land management. This is necessary as the water level fluctuates relative to water-input and water-output within the catchment (Gebre, 2015)

Flood risk is the combination of flood hazards and vulnerabilities at a particular location that needs systematic assessment, collection, and analysis of variables. GIS and its extension (HEC-RAS) have emerged as important device in flood mapping and analysis because it enables the preparation of maps of inundated areas (Adhanom, 2019).

2.11. Flood Mitigation Measure

Mitigation is continued action taken to reduce the risk of flood on property or humans. It refers to a method or progress working to reduce/ avoid the impact of flooding on the communities living in the area. The mitigation activities are working after the flood, during flooding, and before flooding. Flood mitigation measures can be classified into two (Subramanya K. , 2008). Those are:

Structural measure: is a method to control or reduce the flood impacts on the communities by constructing engineering structures. This is used to control floods by using engineering structures like:

- ✚ Storage and detentions reservoir (store the income flood into the reservoir and reduce the flood peak by providing temporary storage by restricting the outlet flow rate)
- ✚ Levees, dykes, or flood embankments (earthen banks constructed parallel to the river courses and the oldest and most commonly used)
- ✚ Floodways (natural channels flood which diverts during peak flood)
- ✚ Channels improvements (increase floodway by widening deepening channel), etc.
- ✚ Land management (developing vegetation and soil covers with land treatment like check dams, contours bund, zing terrace, etc.)

Nonstructural measure: This is the method of flood mitigation which is different from the construction of engineering structures but it follows the method of communities living with the flood. Nonstructural mitigation measures are like:

- ✚ Floodplain zoning (when river discharges high expected that the river over banks and flow into the plain)
- ✚ Relocate (moving the communities will be affected with their assets to the nearest location /area)
- ✚ Flood forecast and early warning (warning to the communities that are affected by flood for appropriate measures)
- ✚ flood insurances (the helping mechanism of communities).

Flood control measure: - flood protection in this case refers to the building levee, dam which is structural flood control measure. Structural measure builds in the flood plain, can counteract flooding of the flood plains in several ways. For example, new catchment dams can reduce flood peak, levee channels the flow into certain predetermined entry ways and flood ways help to channel excessive flow away. But, building and maintenance costs of this type of measure are high (Subramanya K. (., 2009)

Land use measure: Land use planning in flood area has the aim of reducing expected flood hazard on the one hand and reducing the risk of the development in the flood area on the other hand. The different land use options within floodplains would be analyzed. Land use type is dividing into different zones according to river characteristics usually Facilitates the analysis of land use option.

- Land use types are more susceptible to flood than other and the following options can be exercised; the most vulnerable land use land cover activities shall be discouraged in a flood area.
- Land use land cover can be shifted to low vulnerable area, for instance where river has characteristically less flood risk.

2.12. Previous studies

Different researches have undertaken dealing with the application of Hydraulic model by using HEC-RAS in flood hazard and risk assessment (Abu, 2020) used integrated approach of remote sensing and GIS for flood hazard assessment for Ketar river floodplain, located downstream of Abura gauging station in Ziway-dugda woreda, Ethiopia. Abura gauging stations is among the most frequently flood-affected area for which flood risk mapping is so important. The area is situated at the confluence of Katar River it is the main contributor of flood in this area. In order to delineate flood hazard zones, in general, different thematic layers viz., floor of building, age of building, land use, vulnerability map and building material map were developed from topographic sheet and field survey. The study has demonstrated the capabilities of using remote sensing and GIS for detailed mapping of flood hazard zone.

The flood history at the study area is known / experienced by the people living. The upstream of the Awash River basin has been flooded for short duration after intense or prolonged rainfall events, but the downstream area has been flooded for weeks or months every year during wet season. Timing and size of the flood cause influence the production

of the crops cultivated in flood plain. Intense rainfall in the upper Awash River basin occurs at the end of rain season, the flood can damage the crops (Gebre, 2015).

Flood flashing also affect the community below koka reservoir. The people identify flooding coming from Awash River, the surrounding areas and combination of both. Agriculture is the major source of the work for the study area communities and they depend on it for income and for food. The people mostly farm along the Awash River and use irrigation pump for with draw water from Awash River to the irrigation land.

There are types crop growing at the study area. Some of those are; tomato, onion, maize, Cabbage, teff, wheat, barley and etc. all peoples whose living in the study area is affected by flooding. During the rainy season they farming land and grow crop was loses by flood plain because the area is vulnerable to the flood. The highly ranges of flow of the main river and its tributary between the dry and rain season of rainfalls, overflows in the latter cannot used for irrigations and in large measures must be wasted and lost, while in contrast in the dry season there is a shortage of water. Therefore, water control during rainfall season has two main advantages are flood reduce during rainfall season and used during dry season but this method was not applied (Abu, 2020)

The future peak flood forecasting was estimated by using flood frequency analysis (Mokonen, 2021). The flood map done through HEC-GeoRAS and HEC-RAS software's and comparing the amount of crop loss yield produced previously from hectare of land and the expected crop yield from inundated area the flood damage could be estimated (Mokonen, 2021). In this study calibration and validation of hydrological and hydraulic model were didn't worked in this case the output of model might be inaccuracy.

3. MATERIALS AND METHODS

3.1. Description of the area

3.1.1. Locations

The Rift Valley basin is one of the major river basins in Ethiopia and is situated in the central part of the country covering parts of Southern Ethiopia, Central Ethiopia and Oromia Regional States. The study area is located in the central rift valley basin in Central Ethiopia Region Mareko special woreda and Silte Zone. The catchment is geographically bounded between 7°50′–8°13′N and 38°10′–38°32′E, at 108 km from Hossana, Capital city of CER and 5km far from East Mesekan Woreda center, Inseno.

The total area of the Waja watershed is 864.92 km² and was used for hydrologic modeling for this study. Topographically, the Waja watershed is ranging from 1734 m at the outlet near Koshe town to about 3470 m in the high mountainous areas.

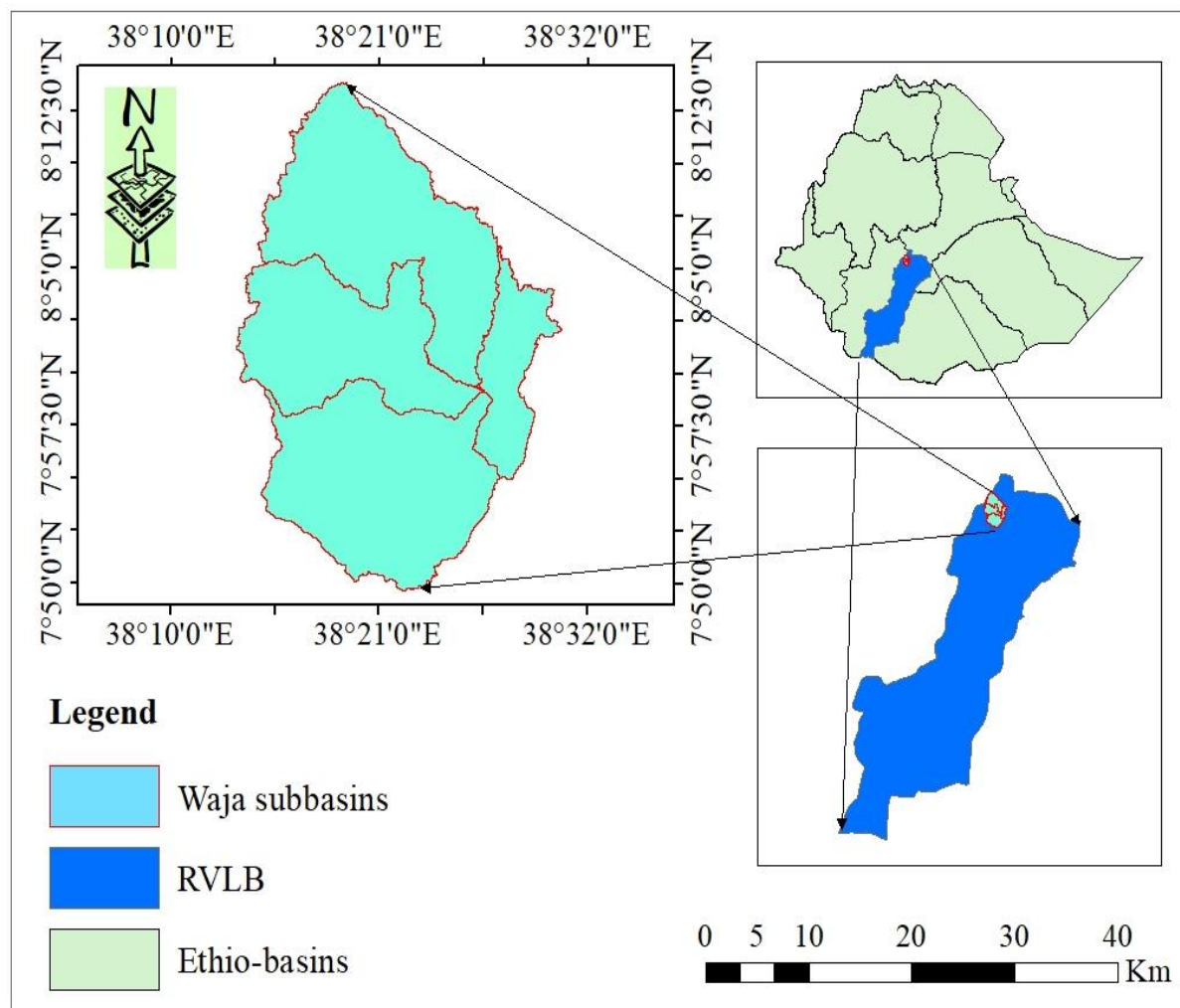


Figure 3.1: Location map of Waja River catchment

3.1.2. Climate

Climate of the study area consists of two ecological zones: humid to dry sub humid, dry sub- humid to semi-arid lands (Makin et al., 1976). Accordingly, highland areas west of Butajira are categorized under humid to dry sub-humid land. The areas north of Butajira around the perennial sources of Waja River are humid to dry sub-humid lands. The rest of the area which is around the watershed is in dry sub- humid to semi-arid zone. Rainfall and temperature in the Waja River catchment strongly varies with the altitude.

The rainfall pattern increase as increasing the altitude from the rift floor to the western highlands. The average annual rainfall varies spatially and ranges from 811 mm/year around the rift floor in the east to 1104 mm/year at extreme highlands areas in the west. Figure 3.2 below shows mean monthly rainfall of three meteorological stations within and around the catchment.

All Three stations have a record from 199-2017 G.C which has more than 27 year's data. From the Figure below, it can be seen that the rainfall distributions are bi-modal. The peak average monthly rainfall appears in the months of June to September while small to moderate rainfall occurs from March to May. The mean annual temperature of Waja ranges from 17.14 to 19.99 °C

3.1.3. Soils

The major soil types in study area exhibit a general relationship with altitude and slopes. The soil types in the study area are classified in to six types known as Chromic Luvisols, Chromic Vertisols, Eutric Cambisol, Marsh, Luvic Phaeozems, and Pellic Vertisols, are generally dominating the area.

Generally, the soils types of this watershed area are characterized with shallow, moderate to deep and very deep in depth and sandy clay to clay texture types. They are reddish brown to red clay soils. Run-off formation from Eutric Cambisol is high and hence it is susceptible to erosion.

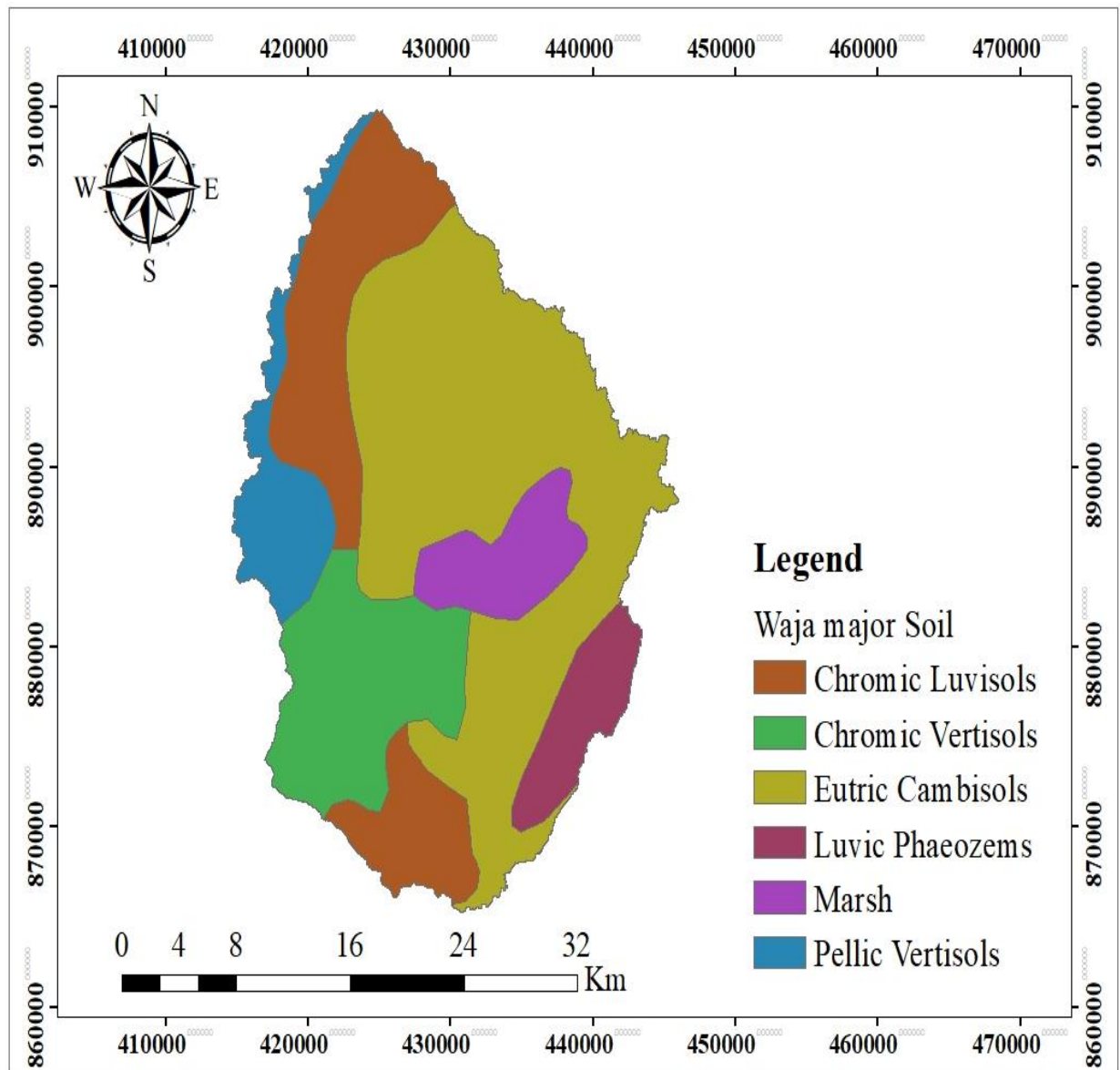


Figure 3.2 : Soil map of the Area

3.1.4. Land Use Land Cover of an Area

The land use and land cover map shows the spatial distribution and classification of various land use types within the study area. By integrating land use and land cover data with soil information, the hydrological characteristics of the region can be effectively assessed. Changes in natural vegetation cover due to cultivation and deforestation have significantly impacted the area, increasing weathering and erosion rates. Additionally, farming activities on slopes have further contributed to soil erosion. The Waja River catchment has experienced extensive damage from sheet erosion, resulting in significant soil loss. Various land use and land cover types are present in the Waja watershed, as shown in Figure 3.4 below, with annual crops being the predominant category.

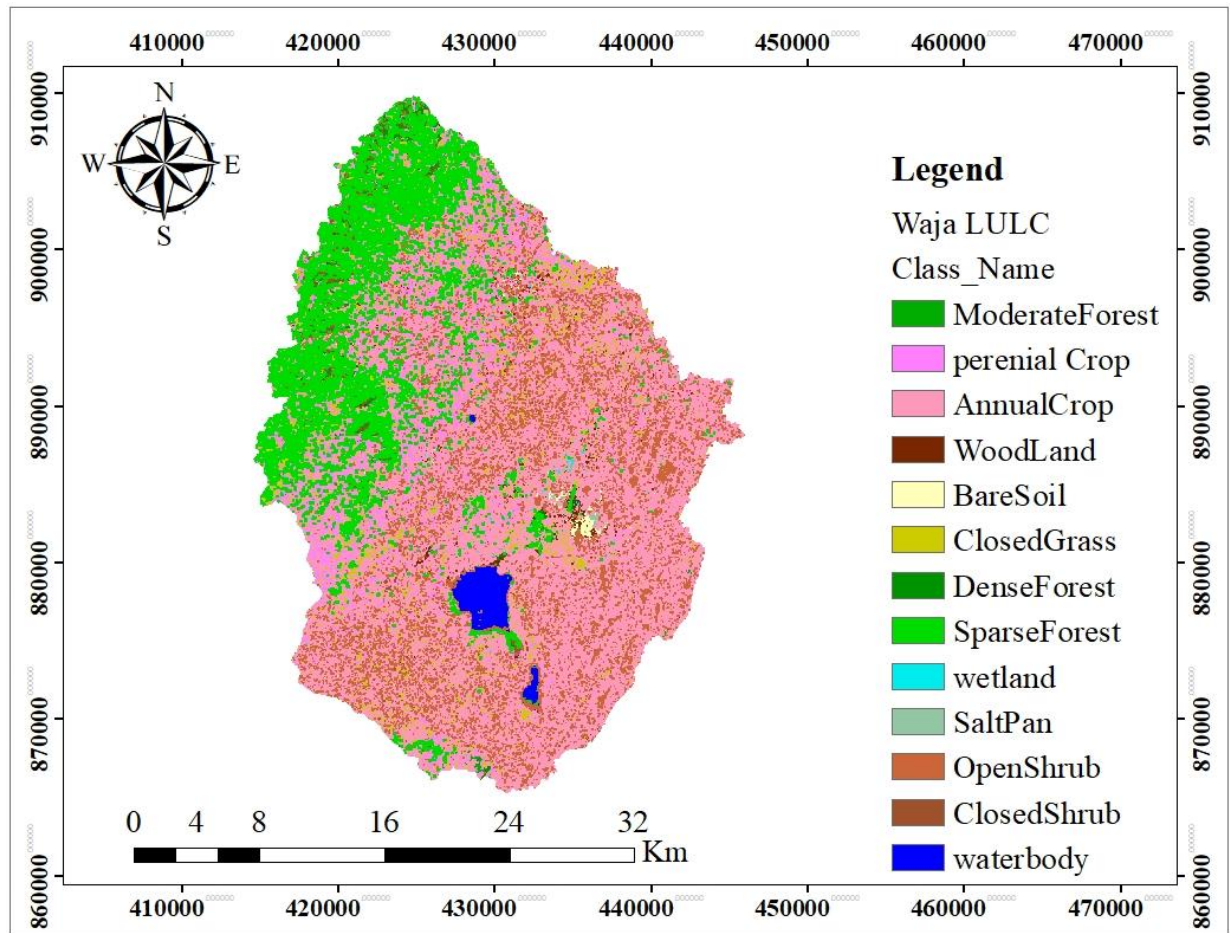


Figure 3.3 : Land use Land Cover map of the Area

3.1.5. Topography of area

The Waja River watershed exhibits a significant elevation range, with altitudes varying from 1,734 meters to 3,470 meters above sea level. This variation in elevation plays a crucial role in shaping the hydrology and geomorphology of the region. In the upper reaches of the watershed, characterized by rugged terrain, the landscape is predominantly defined by convex shapes. These convex slopes typically arise from geological processes such as erosion and sediment deposition, creating undulating landforms that can influence water flow patterns. The steep, rounded contours in this upper region tend to promote rapid surface runoff during rainfall events, leading to increased erosion and sediment transport towards lower elevations. The unique topography of this area is vital for understanding the watershed's hydrological dynamics, as it affects how water is collected, stored, and channeled through the landscape. In contrast, the lower part of the watershed features more linear slope shapes, indicating a gradual transition from the rugged upper terrain to flatter areas. These linear slopes often result from a combination of natural

processes and human activities, such as agriculture and land development. The gentler gradient in this region typically allows for more effective water infiltration and reduced runoff, which can enhance groundwater recharge and support local ecosystems. However, the linear nature of these slopes may also pose challenges, as they can lead to localized flooding if rainfall exceeds the capacity of the soil to absorb water.

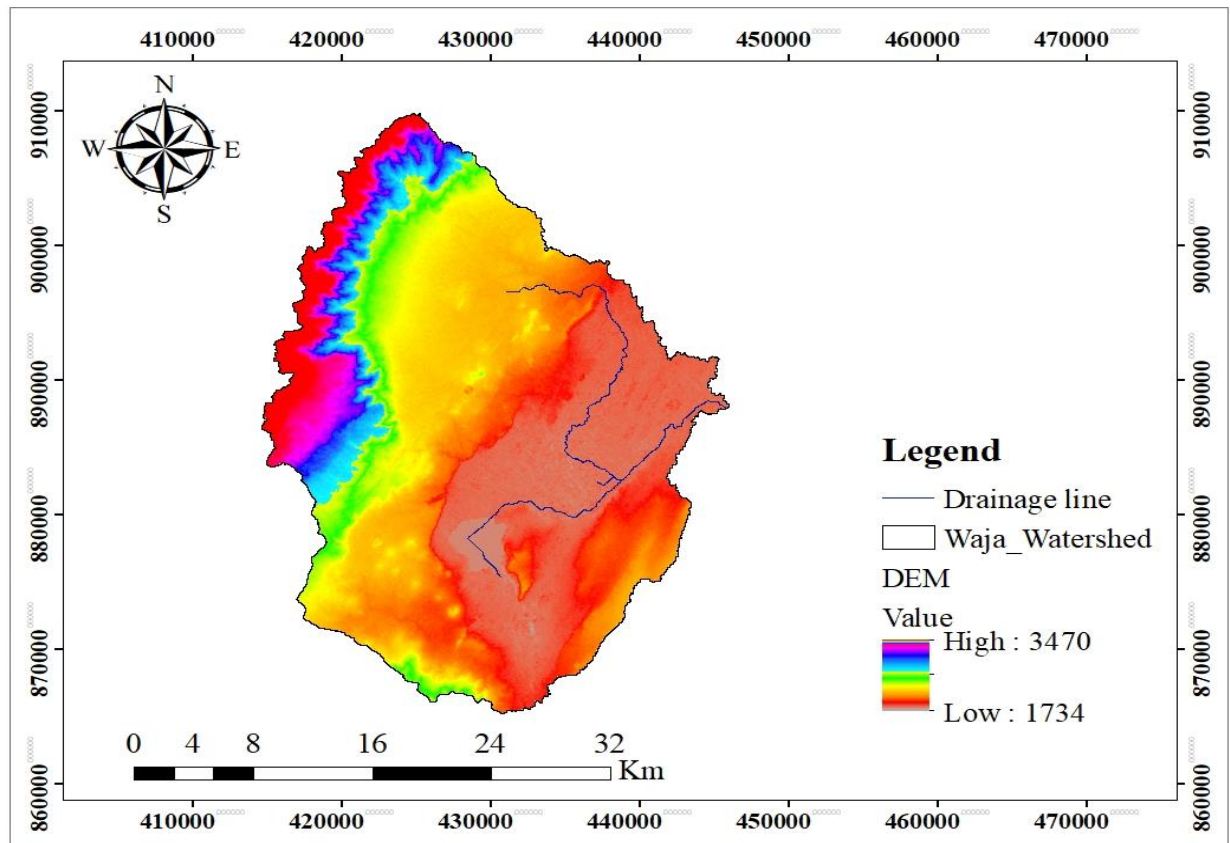


Figure 3.4 : DEM of the study area

3.1.6. Slope of an area

The slope of the watershed plays a critical role in influencing runoff generation, as it directly affects the speed and volume of water that flows over the land during precipitation events. According to the results of terrain analysis based on Digital Elevation Models (DEMs), the slope gradient across the majority of the watershed varies significantly, with values ranging from 0 to 76 degrees. In watersheds where the slope is minimal, typically approaching 0 degrees, water tends to infiltrate the soil more readily, leading to reduced surface runoff, those approaching 76.34 degrees facilitate rapid runoff, as gravity pulls water down the terrain more swiftly. This can result in increased surface water flow, heightened erosion, and a greater potential for flooding. The variation in slope

gradients across the watershed indicates that different areas were respond uniquely to rainfall events. Regions with steep gradients are likely to experience more significant runoff and erosion, which can exacerbate the impacts of flooding and lead to the degradation of soil quality. In contrast, flatter areas may retain more moisture and support vegetation growth, contributing to improved watershed health.

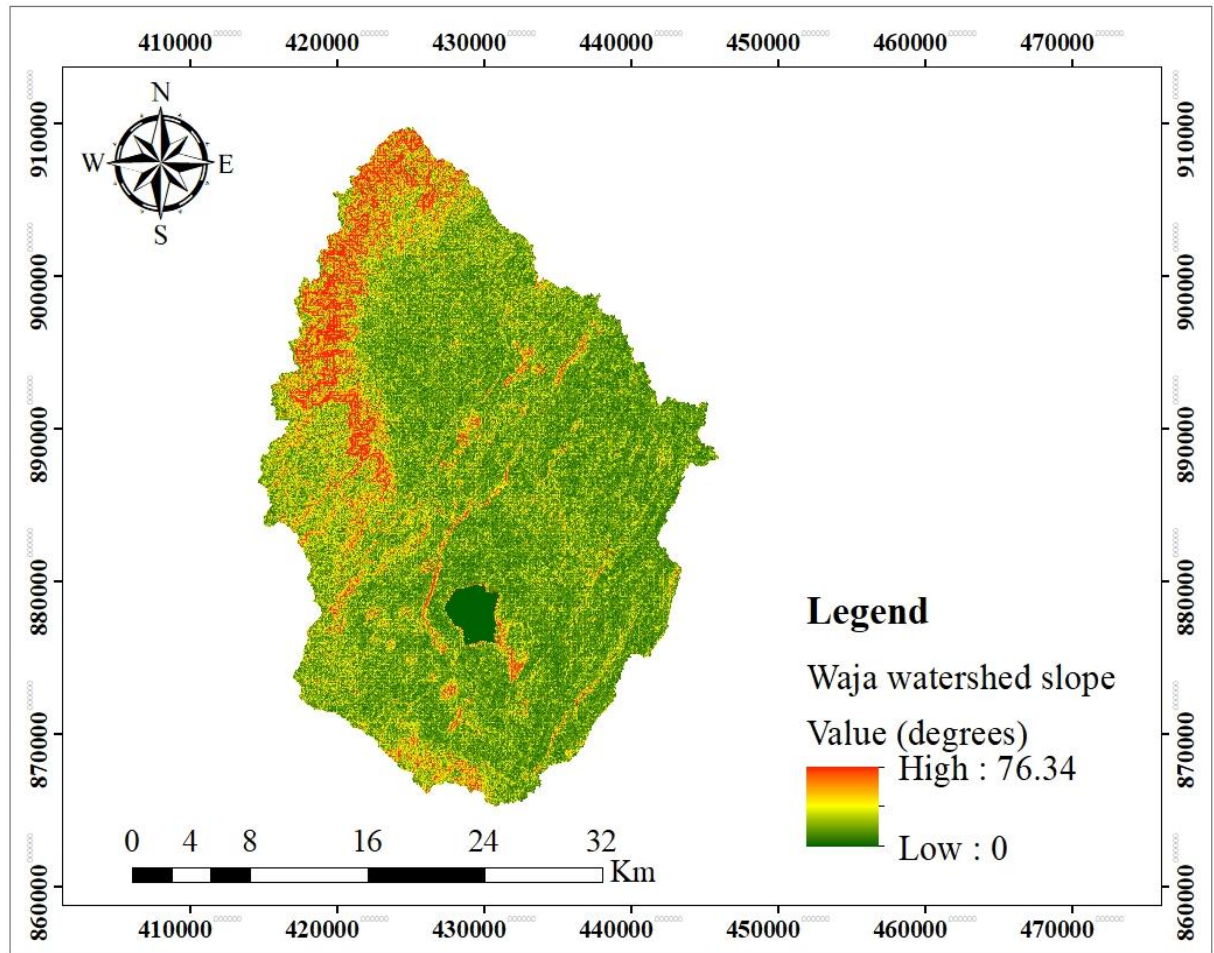


Figure 3.5: Waja Watershed Slope map

3.1.7. Hydrologic characteristics of Waja watershed

The Waja River serves as a vital tributary to Lake Ziway, traversing diverse landscapes as it makes its way to the lake. Throughout its path, the river flows through lush ground forests that are rich in biodiversity and support numerous springs at various locations. This ecological corridor not only provides habitat for various species but also plays a crucial role in maintaining the hydrological cycle of the region. As the River descends through the Zebider Mountains, it approaches the lower reaches of the watershed near Koshe city. However, the river has been undergoing significant changes in its course,

resulting in the erosion and destabilization of its banks. This shifting behavior has profound implications for the local community, particularly for farmers whose agricultural lands lie adjacent to the river. The erosion not only diminishes arable land but also poses a direct threat to local infrastructure, including essential structures such as bridges on the main road to Worabe town, as well as roads and diversion systems designed to manage water flow. The river's loss of guidance and orientation has led to erratic flow patterns, which cover extensive and irregular areas. Consequently, this has resulted in land loss, increased flood damage, and an aesthetically unpleasing landscape. The unpredictable nature of the river raises significant concerns for local residents, who face not only economic challenges due to the loss of farmland but also heightened risks to their safety and property.

3.2.Materials

In this study, the selection of materials and models was carefully determined based on their capacity to address the existing challenges and contribute effectively to achieving the predefined objectives. The integration of appropriate tools and methodologies is crucial for ensuring the reliability and validity of the study results. To fulfill the objectives of the study, the following materials and models were utilized:

- ARC-GIS: - ARC-GIS have been used to delineate watershed area, to know longest flow path, clip soil and LULC maps.
- HEC-HMS was used to simulate the precipitation-runoff processes of the catchment and determine the peak flood discharges for different return period which have been used as an input for HEC-RAS hydraulic model.
- HEC-RAS were used to delineate the flood inundation and hazard map of the study area in concert with Arc-GIS.
- Excel: - Microsoft Excel is used for analyzing different data like climate and stream flow data by using different excel templates.
- GPS:-used to collect the coordinate and elevation data.

3.3. Methods

3.3.1. Data collection

To achieve the objectives of this study, a comprehensive range of data was collected from various sources, ensuring a robust analysis of the hydrological dynamics within the Waja River watershed. The data types gathered include hydro-meteorological data, Digital Elevation Models (DEMs), soil data, land use/land cover information, and socio-economic data.

3.3.1.1. Rainfall data

In this study, rainfall data were collected from three strategically located meteorological stations: Butajira, Koshe, and Tora. These stations were selected for their representative coverage of the Waja River watershed, ensuring a comprehensive understanding of the area's precipitation patterns. The meteorological data were obtained from the National Meteorological Agency (NMA) of Ethiopia, which is known for its extensive network of weather monitoring stations and commitment to providing accurate and reliable climatic information. The dataset spans an extensive period of 30 years, from 1992 to 2021, allowing for a robust analysis of long-term rainfall trends and variability within the watershed.

Table 3.1: Rainfall data stations availability and Location

S/no	Station Name	Region	Woreda	Longitude	Latitude	Station Class	Annual RF
1	Butajira	CER	Meskan	382200	80900	3	1104
2	Koshe	CER	Mareko	383131	80023	4	811
3	Tora	CER	Lanfuro	382514	75120	4	851

3.3.1.2. Hydrological Data

River is gauged at the Butajira outlet. River is the upper reach of Waja River which is part of RVL basin. It is a perennial river that drains an area of 864.92 Km². This data was crucial for model calibration, validation, and analyzing the impacts of meteorological factors on runoff generation and watershed response.

Table 3.2: River Flow stations data availability and Location

River	Site/Location	Catchment	Easting	Northing
Waja	Butajira	RVLB	430451.65	897451.43

3.3.1.3. Digital Elevation Model (DEM)

Digital Elevation Model (DEM) is a square grid of regular spaced elevation data for hydrology, agricultural planning, soil mapping and so on. Unfortunately, the use of DEM surface is generally not suitable for large scale terrain representation for hydraulic analysis of the river channels. Because they cannot vary in the spatial resolution, it may poorly define the land surface in areas of complex relief. Therefore, for hydraulic modeling of river channels, the Digital Elevation Model (DEM) with spatial resolution 12.5m by 12.5 m were downloaded from the Alaska satellite Facility (<https://vertex-retired.daac.asf.alaska.edu/>).

3.4. Data Analysis

3.4.1. Tests on hydrologic data

The basic assumptions in statistical flood frequency analysis are the independence and stationarity of the data series and that the data come from the same distribution homogeneity and outlier, it is better to check the flow data at five percent significance levels to reach an accurate estimate.

3.4.1.1. Test of independence and stationarity

Wald-Wolfowitz (1943) (W-W) test were used to test for the independence of a dataset and to test for the existence of trends in a given sample of size N. For a dataset X_1, X_2, \dots, X_n the statistic R was calculated as;

$$R = \sum_{i=1}^{N-1} X_i X_{i+1} + X_1 X_n \dots \dots \dots (3.1)$$

Where: - X_i – Magnitude of flow at i period

X_{i+1} – Magnitude of flow next to i period

X_1 – Magnitude of flow at first period

X_n – Magnitude of flow at last period

N– Total number of flows

When the elements of the sample are independent, R follows a normal distribution with mean and variance given.

$$\bar{R} = \frac{S_1^2 - S_2}{N - 1} \dots \dots \dots (3.2)$$

$$Var(R) = \frac{S_1^2 - S_2}{N - 1} - \bar{R}^2 + \frac{S_1^4 - 4S_1^2S_2 + 4S_1^2S_3 + S_2^2 - 2S_4}{(N - 1)(N - 2)} \dots \dots \dots (3.3)$$

Where; $S_r = Nm'_r$ and $m'_r = \frac{1}{n} \sum_{i=1}^n x_i^r$

m'_r is the rth moment of the sample about the origin

The statistic U is approximately normally distributed with mean zero and variance unity. In this thesis, the test of independence was at 5 % significance level, by comparing the statistic u with the standard normal variate $u_{a/2}$ corresponding to a probability of exceedance $a/2$.

$$U = \frac{R - \bar{R}}{\sqrt{Var(R)}} \dots \dots \dots (3.4)$$

3.4.1.2. Tests of homogeneity and stationarity

The Mann- (Whitney, 1947) test considers the quantities V and W by testing two samples of size p and q, where p is less than or equal to q are compared. The combined data set of size $N = p + q$ was ranked in increasing order.

$$V = R - \frac{(P(P + 1))}{2} \dots \dots \dots (3.5)$$

$$W = pq - V \dots \dots \dots (3.6)$$

R is the sum of the ranks of the elements of the first sample (size p) in the combined series (size N), V and W are calculated from R, p, and q. V represents the number of times an item in sample 1 follows an item in sample 2 in the ranking. Similarly, W can be computed for sample 2 following sample 1. The M-W statistic U will be defined by the smaller of V and W. When $N > 20$ and $p, q > 3$, and under the null hypothesis that the two samples came from the same population, U is approximately normally distributed with mean and variance var (U),

$$\bar{U} = \frac{pq}{2} \dots \dots \dots (3.7)$$

$$Var(U) = \frac{pq}{N(N-1)} \left(\frac{N^3 - N}{12} - \sum T \right) \dots \dots \dots (3.8)$$

$$T = \frac{J^3 - J}{12} \dots \dots \dots (3.9)$$

Where T and J is the number of observations tied at a given rank. T is summed over all groups of tied observations in both samples of size p and q. Therefore, in this thesis the statistic u is used to test the hypothesis of homogeneity at 5 % significance level a by comparing it with the standard normal variety for that significance level.

$$u = \frac{U - \bar{U}}{\sqrt{Var(U)}} \dots \dots \dots (3.10)$$

3.4.1.3. Testing of outliers

Outliers are data points that depart significantly from the trend of the remaining data. The retention or deletion of this outlier can significantly affect the magnitude of statistical parameters computed from the data; especially for small samples procedures for trending outliers require judgment involving both mathematical and hydrological considerations. According to the (Jekel et al., 2014) if the station skew is bigger than +0.4 tests for high outliers are considered first; if station skew is less than -0.4, test for low outlier are considered first. Where the station skew is between -0.4 and +0.4, tests for both high and low outlier should be applied before eliminating any outliers from the data set. The following frequency equation can be used to detect high outliers.

$$Y_h = \bar{Y} + K_n S_y \dots \dots \dots (3.11)$$

Where: Y_h = High outlier threshold in log units,

K_n = Value read from table for sample size n

S_y = Standard deviation

$$S_y = \sqrt{\frac{\sum(Y_i - \bar{Y})^2}{n-1}} \quad , \quad Q_H = (10)^{y_h}$$

A similar equation can be used to detect low outliers

$$Y_L = \bar{Y} - K_n S_y \dots \dots \dots (3.12)$$

If the logarithms of the values in a sample are bigger than Y_h in the above equation, then it is considered high outlier. Flood peaks considered high outliers should be compared with historic flood data and flood information at nearby sites. Historic flood data comprise information on unusually extreme events outside of the systematic record. According to the (Jekel et al., 2014) if information is available that indicates a high outlier is the maximum over an extended period of time, the outlier is treated as historic flood data and excluded from analysis. If useful historic information is not available to compare to high outliers, then the outliers should be retained as part of the systematic record.

3.4.2. Consistency checks and Adjustment of Rainfall Data

When dealing with inconsistent catchment rainfall data over time, it becomes necessary for hydrologists to correct or adjust the measured data to ensure a consistent record. Inconsistency in the data can arise from various factors such as changes in gauge location, exposure, instrumentation, or issues with the observational procedure. To address this problem, one widely applied technique is the Double-Mass Curve (DMC) analysis. The DMC analysis is a graphical method that compares the time trends of a particular station's record with those of nearby stations. It helps identify and adjust inconsistencies in the data. The DMC analysis involves plotting cumulative rainfall data for the station of interest against cumulative rainfall data from a reference station or a group of nearby stations. The cumulative rainfall is calculated by summing up the rainfall values over a specific period, such as yearly or monthly totals. By comparing the slopes and patterns of the two curves on the graph, inconsistencies or shifts in the time trends can be detected. If the curves of the station of interest and the reference station(s) exhibit similar patterns and slopes, it suggests a consistent record. However, if there are significant deviations or shifts between the curves, it indicates inconsistencies that need to be addressed.

The DMC analysis helps in identifying potential causes of inconsistency, such as changes in gauge location or exposure. Based on the analysis, adjustments can be made to the data by applying scaling factors or shifting the data to align the time trends with the reference station(s). This process helps create a more consistent record for further hydrological analysis and modeling. After the data of each station are arranged in descending order, the accumulative sums, station to be investigated and base station; are plotted against

each other and line of best fit were sketched as shown on figure 3.6 below. The data series, which is inconsistent, adjusted to consistent values by proportionality.

$$P_{cx} = P_x * \frac{M_c}{M_a} \dots\dots\dots (3.13)$$

- ❖ Where P_{cx} is corrected precipitation at any time period and P_x is original recorded precipitation at time period
- ❖ M_c is corrected slope of double mass curve and M_a is original slope of the double mass curve

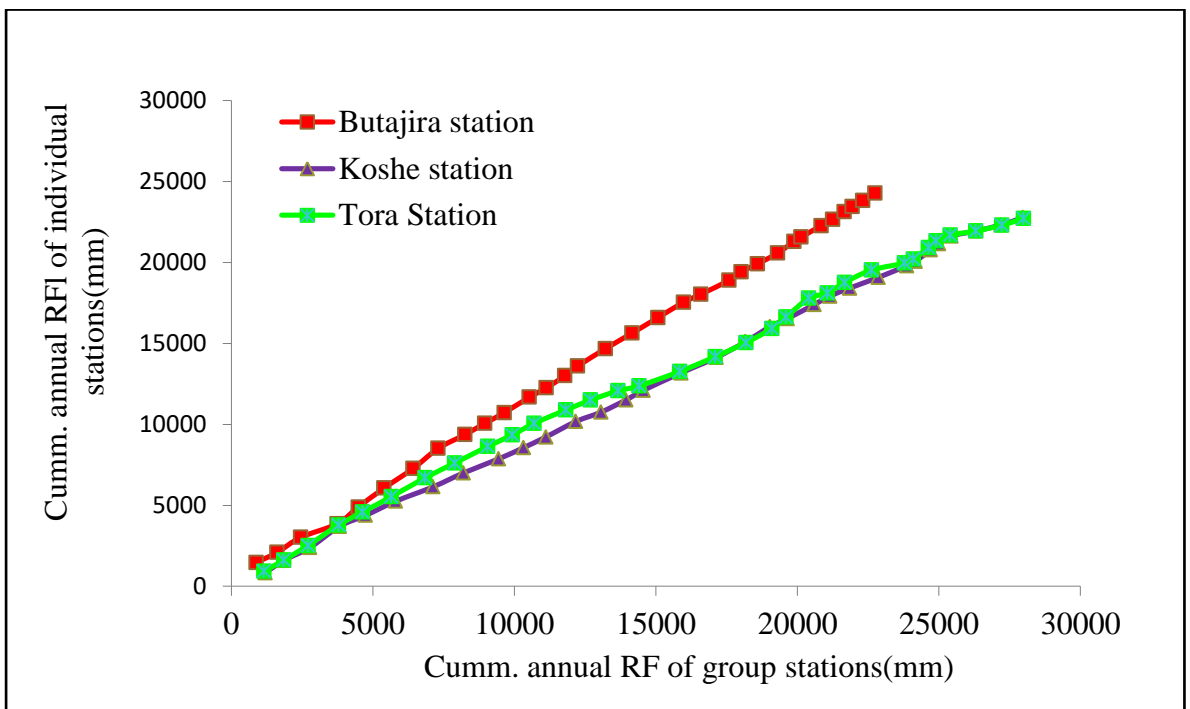


Figure 3.6: Double mass curve

3.4.3. Goodness of fit test

This test helps to determine how well a specific distribution fits hydrological data and provide insights into the appropriateness of the chosen distribution. The D-index is a criterion used to select a suitable probability distribution for rainfall estimation.

It is calculated using Equation 3.14,

$$D\text{-index} = \left(\frac{1}{\bar{R}}\right) \sum_{i=1}^6 [R_i - R_i^*] \dots\dots\dots (3.14)$$

Here, \bar{R} is the average value of the series of the recorded rainfall, R_i (for $i=1$ to 6) are the six highest values in the series of recorded rainfall and R_i^* is the estimated rainfall by

probability distribution. The distribution having the least D-index is considered as the better suited distribution for rainfall estimation (USWRC 1981). To determine the most suitable distribution, the D-index values are computed for different distributions, and the distribution with the lowest D-index is considered the best fit for rainfall estimation. In this case, the D-index values for various distributions were calculated and presented in Table 3.3. Upon analyzing the table, it can be observed that the D-index value obtained from the normal distribution is the lowest among the compared distributions, including Log-normal, Log-Pearson Type III, Gumbel EVI, Pearson type III, and Gumbel distributions. This implies that the normal distribution is the best suited distribution for rainfall estimation based on the D-index criterion. The D-index provides a quantitative measure to assess the goodness-of-fit of different probability distributions for rainfall data. By comparing the D-index values, hydrologists can determine the distribution that closely matches the characteristics of the recorded rainfall data. In this case, the normal distribution exhibited the lowest D-index, indicating its superior fit for the rainfall data under consideration.

Table 3.3: D-index values of different distributions

Distributions	Normal	Log Pearson Type III	Log Normal	Pearson Type III	Gumbel EVI	Gumbel
D-Index value	0.236	0.259	0.505	0.258	0.450	2.688

3.4.4. Determination of Areal Rainfall

To determine the areal rainfall over a catchment, various methods can be employed. One commonly used method is the Thiessen polygon method, which is also utilized in this particular study. The Thiessen polygon method assigns weights to different rain gauges based on their areal coverage of the watershed. This approach eliminates discrepancies caused by variations in gauge spacing throughout the basin.

The method considers all the stations within and around the basins, assuming a linear variation in precipitation between adjacent gauge stations. To implement the Thiessen polygon method, areas and lines are drawn on a map of the area using ArcGIS 10.3 software with the Arc toolbox extension. The lines connect adjacent gauge stations, and the perpendicular bisectors of these lines form a pattern of polygons, with each polygon

containing one gauge station. The area of each polygon represents the area associated with that station and is used as a weighting factor for the station's precipitation. By applying this method, the contribution of rainfall from each gauge station is limited by its weighting factor. This allows for the estimation of average precipitation over the catchment, considering the spatial distribution of the rain gauges.

According to Thiessen, the average rainfall, R_{areal} , over the area can be computed from equation

$$R_{Areal} = \sum_{i=1}^n \frac{R_i * A_i}{A_t} \dots\dots\dots (3.15)$$

Where R_i is the rainfall at station i_{th} , A_i is the polygon area of station i_{th} , A_t is the total catchment area, and n is the number of stations. The area functions A_i/A_t are known as the Thiessen coefficients and once they are determined for a given stable station network, the areal rainfall can be computed for the set of rainfall measurements. The three nearby location of the rainfall stations are as shown below.

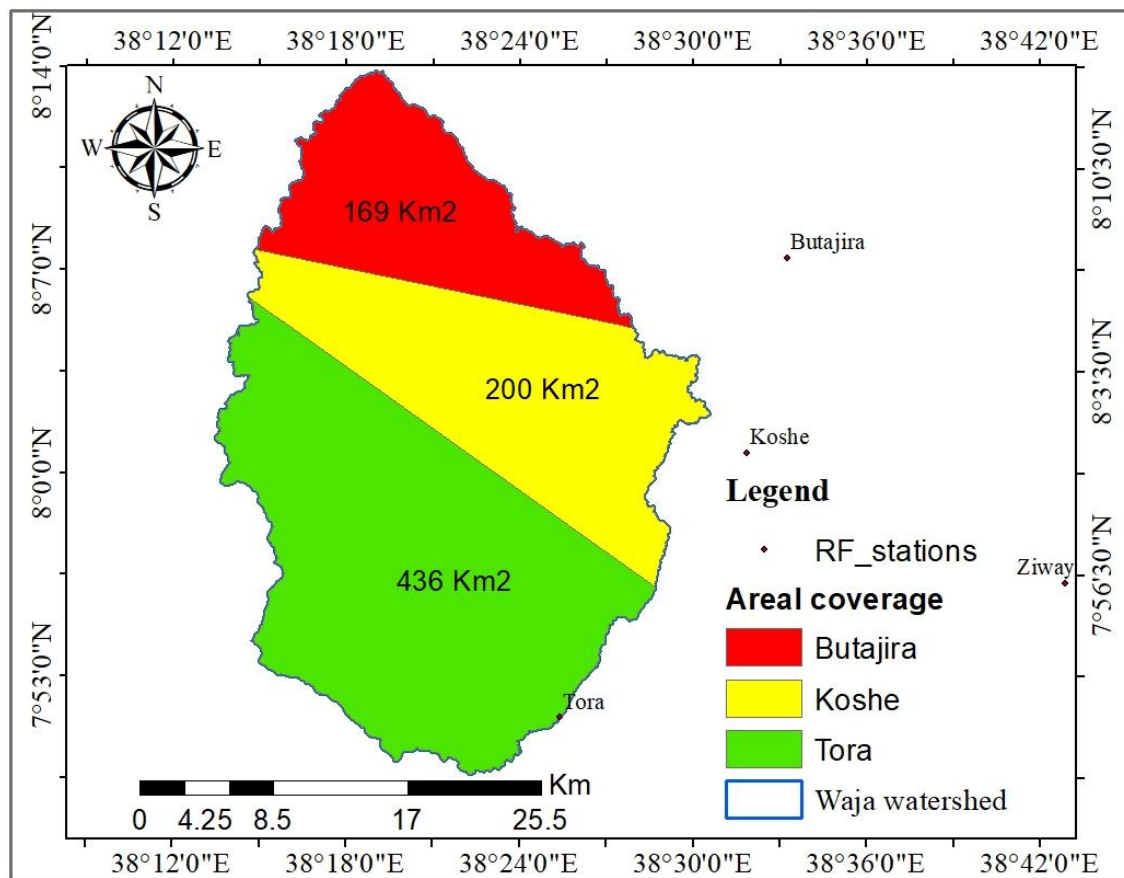


Figure 3.7: Area coverage of Rainfall Stations

3.5. Hydrological modeling using HEC-HMS model

HEC-HMS is a semi distributed model, in which data can be heterogeneous within basin but it is homogenous within sub-basins. The hydrological characteristics of the basin have been computed using the physical properties of all the sub basins for simulation. The Hydro-meteorological data and curve number for each sub basins has been required for simulation of the model. To perform rainfall-runoff modeling with HEC-HMS, several input files are required:

- Background Map File: This file provides the spatial information and characteristics of the study area. It includes data such as the boundaries of the catchment, topography, land use, and other relevant features.
- Basin Model File: The basin model file contains the hydrological characteristics and parameters of the catchment being modeled. It includes information on soil types, land use categories, vegetation, and flow routing methods.
- Gage File: The gage file includes observed precipitation and/or stream flow data, which are used for calibration and validation of the model. This data is typically obtained from rain gauges or stream gauges located within the study area.
- Met File: The met file contains meteorological data required for the rainfall-runoff simulation. It includes information such as precipitation, temperature, humidity, wind speed, and solar radiation. These data are used to estimate actual evapotranspiration and calculate potential evapotranspiration using different methods.

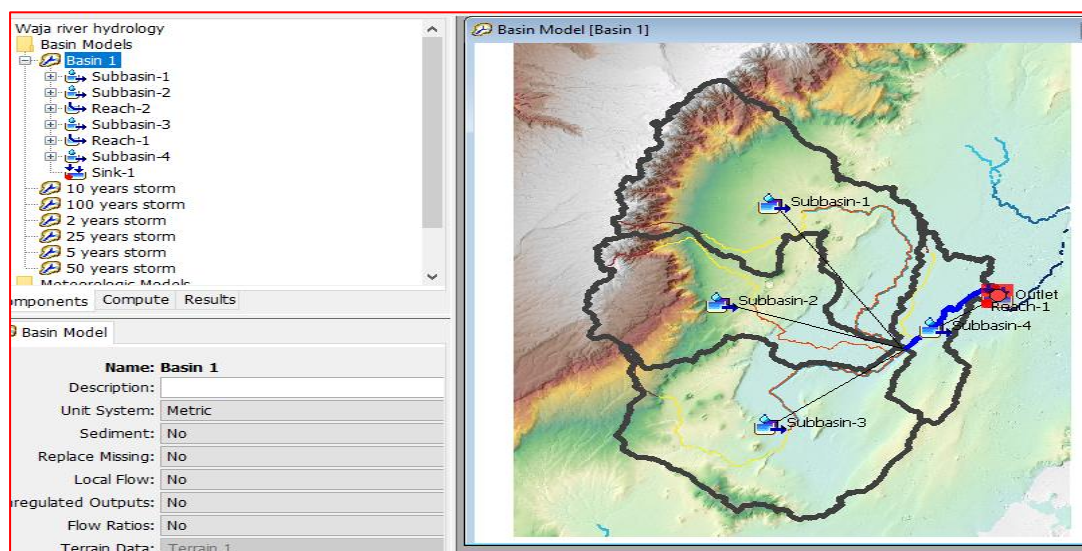


Figure 3.8: Waja river watershed in HEC HMS model

HEC–HMS consists of different methods for precipitation loss modeling; The SCS Curve Number (SCS-CN) model is a commonly used method within the HEC-HMS software for estimating excess precipitation or direct runoff from a storm event. It was developed by the Soil Conservation Service (SCS), now known as the Natural Resources Conservation Service (NRCS), in 1972. The SCS-CN model takes into account various factors such as cumulative precipitation, soil type, vegetation, and antecedent moisture condition of the watershed to estimate the depth of excess rainfall or direct runoff.

The computation of excess precipitation or direct runoff using the SCS-CN model is based on the following equation:

$$Q = \frac{(P-0.2S)^2}{P+0.8S} \dots\dots\dots (3.16)$$

Where:

Q = Depth of excess precipitation or direct runoff (in inches)

P = Cumulative precipitation (in inches)

S = Potential maximum retention after runoff begins (in inches)

In the SCS Curve Number (SCS-CN) model, the potential maximum retention (S) is related to the Curve Number (CN) and can be calculated using the following equation:

$$S = \frac{25400-254 \text{ CN}}{\text{CN}} \dots\dots\dots (3.17)$$

Where:

S = Potential maximum retention after runoff begins (in inches)

CN = Curve Number

In a watershed with different land uses and soil types, a composite Curve Number (CN) can be calculated to estimate the runoff volume. The composite CN represents an average value that considers the contributions of individual watershed subdivisions with homogeneous land use and soil type. The equation to calculate the composite CN is as follows:

$$CN_{\text{composite}} = \frac{\sum A_i \text{ CN}_i}{\sum A_i} \dots\dots\dots (3.18)$$

Where:

CN composite = Composite Curve Number used for runoff volume estimation

i = Index of each watershed subdivision with homogeneous land use and soil type

CN_i = Curve Number of the watershed subdivision i

A_i = Drainage area of the subdivision i

The resulting value, CN composite, represents the average Curve Number for the entire watershed, taking into account the variations in land use and soil type. This composite CN can be used in the SCS-CN model or other runoff volume estimation methods to simulate the runoff process and estimate the total runoff volume more accurately. The model allows the transformation of excess precipitation into direct runoff. The SCS (Soil Conservation Service) unit hydrograph model is commonly used as a transform model in the Hydrologic Engineering Center's Hydrologic Modeling System (HEC-HMS) for certain watersheds due to its simplicity, wide applicability, and historical significance.

In SCS unit hydrograph model, which is used as a transform model to convert excess precipitation into point runoff, the following relationships and equations are used:

Relationship between UH peak (U_p) and time to UH peak (T_p):

$$U_p = C \frac{A}{T_p} \dots\dots\dots (3.19)$$

Where:

U_p = Peak discharge of the unit hydrograph (in cubic feet per second)

A = Watershed area (in acres)

C = Conversion constant (2.08) - This constant is used to convert the U_p to the desired units based on the unit of A (acres) and T_p (hours)

T_p = Time to the UH peak (in hours)

This relationship allows for the estimation of the peak discharge of the unit hydrograph based on the watershed area and the time to the peak. Relationship between the time to UH peak (T_p) and the duration of the unit of excess precipitation (Δt) and basin lag (t_{lag}):

$$T_p = \frac{\Delta t}{2} + t_{lag} \dots \dots \dots (3.20)$$

Where:

Δt = Duration of the unit of excess precipitation (in hours)

T_{lag} = Basin lag (in hours)

Basin Lag time in hours for each sub-basin was computed using equation (3.11) (Arlen, 2000) and then converted to minutes.

$$Lag = \frac{L^{0.8} (S+1)^{0.7}}{1900 * Y^{0.5}} \dots \dots \dots (3.21)$$

Where S = Maximum retention

Lag = basin lag time (hours)

L= hydraulic length of the watershed (longest flow path)

Y = Basin slope (%).

The model includes several methods for channel flow routing. Among those models, the Muskingum model for flood routing was selected for this study due to the availability of required data. The Muskingum method uses a simple finite difference approximation of the continuity equation:

$$\left(\frac{I_{t-1} + I_t}{2}\right) - \left(\frac{O_{t-1} + O_t}{2}\right) = \left(\frac{S_t + S_{t-1}}{\Delta t}\right) \dots \dots \dots (3.22)$$

Storage in the reach is modeled as the sum of prism storage and wedge storage. The storage is defined by the model as:

$$S_t = K O_t + K X (I_t - O_t) = K [X I_t + (1 - X) O_t] \dots \dots \dots (3.23)$$

Where K = travel time of the flood wave through routing reach, and X = dimensionless weight ranging from 0 to 0.5. The quantity $X I_t + (1 - X) O_t$ is a weighted discharge. When the storage in the channel is controlled by downstream conditions, such that storage and outflow are highly correlated, X=0.0. Thus, $S = K O$ and it is the linear reservoir model. If X=0.5, the inflow, and outflow have the same weight which means that the

wave does not attenuate when moving through the reach. By substituting equation (2.9) in (2.8) and rearranging to isolate the unknown values at time t, we have:

$$O_t = \left(\frac{\Delta t - 2KX}{2K(1-X) + \Delta t} \right) I_t + \left(\frac{\Delta t + 2KX}{2K(1-X) + \Delta t} \right) I_{t-1} + \left(\frac{2K(1-X) - \Delta t}{2K(1-X) + \Delta t} \right) \dots\dots\dots (3.24)$$

3.5.1. Basin characteristics

Basin characteristics refer to the physical and hydrological properties of a watershed or catchment area. These characteristics play a crucial role in understanding and modeling the behavior of the basin's hydrological processes. Some important basin characteristics include Curve Number (CN), Basin Lag Time, basin area, Basin Slope, Potential Maximum Retention (S).

Table 3.4: Basin parameters of Waja watershed

Sub basins	L(Km)	Basin slope	Basin Area(Km ²)	CCN	Tlag(Min)	Ia(mm)
Subbasin-1	53.13	0.17639	293.59	75.1	326.76	16.88
Subbasin-2	37.91	0.15827	207.38	75.1	262.76	16.80
Subbasin-3	46.31	0.09178	282.33	75.6	399.89	16.42
Subbasin-4	27.02	0.03925	81.623	78.6	362.88	13.80

3.5.2. Calibration and Validation of the Model Parameters

After the model setup is completed for HEC-HMS model, the next step is to run the model and analysis the simulated result. The applicability of the model for intended purpose should be evaluated through the process of sensitivity analysis, calibration and validation (White and Choubey, 2005). For further analysis of the result, model calibration involves modification of input parameters and comparison of predicted output with observed values until the defined objective function is achieved (James and Burges, 1982). And the calibration was carried out by trial and error where model parameters are manually or automatic calibration. In order to utilize the calibrated model for estimating the effectiveness of future potential management practices, the model tested against an independent set of measured data. This testing of a model on an independent set of data set is commonly referred to as model validation. As the model predictive capability was demonstrated as being reasonable in both the calibration and validation phases, the model is used for future predictions under different management scenarios (Ashenafi, 2013). Daily rainfall and stream flow data

from 1996 to 2010 were used for calibration and validation of the model. The data from 1996 to 2005 were used during calibration and from 2006 to 2010 was used during validation.

3.5.3. Model Performance Evaluation Criteria

Performance measurement allows for visual comparison of data from simulated and measured output responses, helps to identify model bias, identify variations in peak timing and magnitude (e.g. peak flows) and recession curve shape, etc. (Moriassi, 2015). The performance of the HEC–HMS model was evaluated on four performance assessment parameters. These are Nash Sutcliff Efficiency (NSE), determination coefficient (R^2), root mean square error (RMSE) and percent bias (PBIAS).

Nash–Sutcliffe model efficiency coefficient (NSE): used to analyze the correlation between simulated and observed hydrological data. It can range from $-\infty$ to 1. An efficiency of 1 indicates a correct match of simulated (modeled) discharge to the measured (observed) data. The efficiency of 0 shows the model prediction is as perfect as of the average of the observed data, whereas the efficiency less than zero occur when the observed average is a better predictor than the modeled or, in another word, when the residual variances (expressed by a nominator) is greater than the data variances (expressed by a denominator). Essentially, the closer the model efficiency is to 1, the more accurate it is. The disadvantage of this efficiency criterion is an overestimation of the model performance during peak-flows and an underestimation during the low-flow condition. It can be expressed as follow:

$$NSE = 1 - \frac{\sum_{i=1}^n (Q_{si} - Q_{oi})^2}{\sum_{i=1}^n (Q_{oi} - \bar{Q}_o)^2} \dots\dots\dots (3.25)$$

Where, Q_{si} - Simulated flow value at the i th time interval, Q_{oi} - Observed flow value at the i th time interval, \bar{Q}_o - Mean observed flow value

Coefficient of Determination (R^2): The coefficient of determination is a measure of the proportion of variances of the forecasted outcomes. It estimates how well the dispersion of the measured data is predicted by the model. With a value of 0-1, the coefficient of determination is computed as the square of the correlation coefficients (R) between the sample and forecasted (predicted) data. The coefficient of determination indicates how well a regression model fits the data. A value of 1 shows every point on the regression

lines fit the data; a value of 0.5 shows only half of the variations are discussed by the regression. A zero coefficient of determination (R^2) indicates that the dependent variable cannot be forecasted from the independent variable. The equation of coefficient of determination can be expressed as follow:

$$R^2 = \frac{\sum_{i=1}^n (Q_{si} - \bar{Q}_s)(Q_{oi} - \bar{Q}_o)^2}{\sum_{i=1}^n (Q_{si} - \bar{Q}_s)^2 \sum_{i=1}^n (Q_{oi} - \bar{Q}_o)^2} \dots\dots\dots (3.26)$$

Where Q_{si} - Simulated flow value at the i th time interval, Q_{oi} - Observed flow value at the i th time interval, \bar{Q}_o - Mean observed flow value, \bar{Q}_s - Mean Simulated flow value.

3.5.4. Flood Frequency Analysis

Flood Frequency Analysis (FFA) is a critical statistical method used to understand the characteristics and magnitude of peak flows in rivers or floodplains. It provides a probability model curve that relates the frequency of occurrence of a flood peak to its magnitude. This analysis is based on historical flood data and observations collected over a specific period. After calibrating and validating the hydrological model using observed flow data, the next step was to estimate the maximum annual rainfall for durations other than the available 24-hour data. Thus, by analyzing the peak annual rainfall data recorded over a period of 30 years (1992-2021), FFA allows for the estimation of return periods. The ERA Drainage Manual 2013 introduced an equation that was utilized to estimate the maximum annual rainfall for various durations based on the available 24-hour maximum rainfall data. This equation assumes a relationship between the 24-hour maximum rainfall and the maximum rainfall for different durations. By applying this equation, the maximum annual rainfall values for selected durations, such as 1-hour, 2-hour, 6-hour, or any other desired duration, were calculated. These estimates were derived from the observed 24-hour maximum rainfall data. Using the provided equation from the ERA Drainage Manual 2013, the annual maximum rainfall depths were computed for each selected duration. This allowed for the estimation of rainfall intensities for different durations, which is crucial for understanding the potential for intense rainfall events and their impact on hydrological processes. It is important to note that the specific equation from the ERA Drainage Manual 2013 is likely based on extensive analysis of rainfall data and regional characteristics. The coefficients or formulas within the equation take into account factors such as climate patterns, geographical location, and statistical analysis of

rainfall data. By utilizing this equation, it becomes possible to estimate the maximum annual rainfall depths for various durations,

$$R_{Rt} = \frac{t}{24} \frac{(b+24)^n}{(b+t)^n} \dots\dots\dots (3.27)$$

Where:

R_{Rt} = Rainfall depth Ratio R_t : R_{24}

R_t = Rainfall depth in a given duration's t .

R_{24} = 24 hr. rainfall depth b and n = coefficients $b=0.3$ and $n= (0.78-1.09)$.

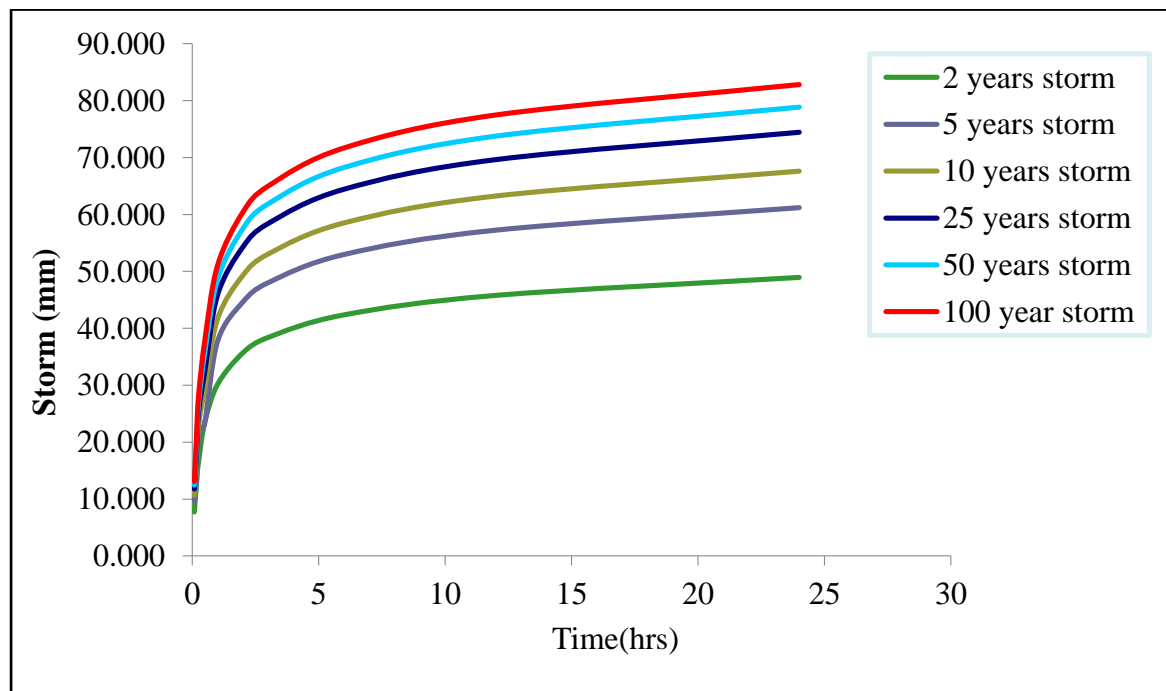


Figure 3.9: Frequency storm depth

3.6. Hydraulic Modeling Using HEC RAS model

The full unsteady flow equations have the capability to simulate the widest range of flow situations and channel characteristics. The basic data requirements for hydraulic routing techniques include: flow data, channel geometry, roughness coefficients, and the boundary conditions. Unsteady flow analysis was used to evaluate the downstream attenuation of the flood wave, providing a more accurate estimate of flood magnitude and velocity at critical locations.

3.6.1. Mesh Generation

The accuracy of the HEC RAS result is dependent on the terrain of the study area. Mesh of narrow size for good accuracy was developed for simulation used in geometric data editor. In the current study area, mesh size of 15m * 15 m was used for simulation. Figure below shows the mesh generated in geometric data window of HEC-RAS model.

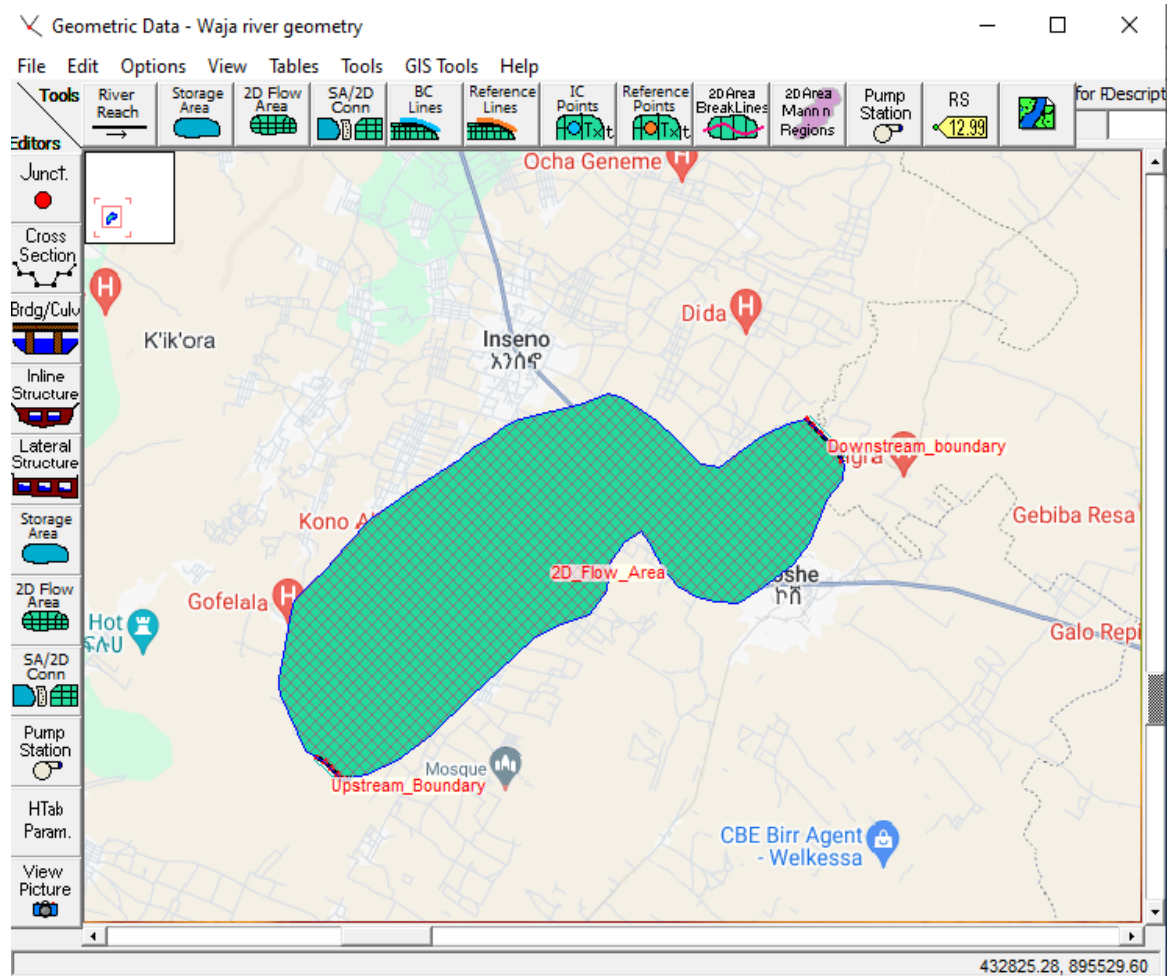


Figure 3.10: Mesh generation within 2D Area

3.6.2. Manning's roughness coefficient

The manning's roughness coefficient is used to reflect the resistance to flow from bed material. The roughness of a surface affects the characteristics of runoff, whether the water is on the surface of the watershed or in the channel. With respect to the hydrologic cycle, the roughness of the surface retards the flow. For overland flow, increased roughness delays the runoff and increase the potential for infiltration. Reduced velocities associated with increased roughness should also decrease the amount of erosion (Gilley et

al., 1991). All hydraulic computations involving flow in open channels require an evaluation of the roughness characteristics of the channel. The ability to evaluate roughness coefficients must be developed through experience. One means of gaining this experience is by examining and becoming familiar with the appearance of some typical channels whose roughness coefficients are known (Bahramifar et al., 2013). Common methods of estimating Manning's roughness coefficients for stream channels, includes use of published n - value data, comparison with photographs of channels for which n values have been computed, and n - value equations (Coon, 1997). A Manning n will be assigned in accordance with a simple land cover classification that will be manually created from parcel outlines and digital orthophotos, using Chow's (1959) tabular n values for similar land characteristics (Gallegos et al., 2009). The roughness Manning n values for different land uses are provided on Chow's (1959). It could also be selected based on reviewing the site visit, photographs and aerial imagery of channel and flood plain areas (Asnaashari et al., 2014). The Manning's coefficients for the channel and overbank areas have been estimated based on the field investigation (Changzhi et al., 2014).

3.6.3. External 2D Flow Area Boundary conditions unsteady simulation

Boundary conditions both at the upstream and downstream ends of study area are needed for the model in flood routing. There are five types of external boundary conditions that can be linked directly to the 2D flow areas. These are Flow Hydrograph, Stage hydrograph, Normal depth, Rating curve and Precipitation boundary condition. The Normal depth and rating curve boundary condition can only be used at locations where flow will leave a 2D flow area. The flow and stage Hydrograph boundary condition can be used for putting flow into or taking flow out of a 2D flow area.

Unsteady flow data used as a boundary condition in this study are: 10years inflow hydrograph, 25 years inflow hydrograph, 50 years inflow hydrograph, 100 years inflow hydrograph and Normal depth. Normal depth is used as a downstream boundary condition. Normal depth can only be used as a downstream boundary condition for an open-ended. To use normal depth, it is required to enter a friction slope for the reach in the vicinity of the boundary condition. The slope of the water surface is often a good estimate of the friction slope. In addition to the boundary condition, initial condition should be established at the beginning of the unsteady flow simulation. Initial condition consists of flow and stage information at each of the cross sections, as well as elevations for any storage areas defined in the system. Once the terrain development steps are

complete, the 2D simulation is executed in HEC-RAS. The software solves the 2D Saint-Venant equations using the selected computational method (e.g., Full Momentum or Diffusion Wave) to simulate the flow behavior and water surface elevations within the defined area.

3.6.4. Post Processor

The post processor is used to compute detailed hydraulic information for a set of user specified time lines during the unsteady flow simulation period. The Post processor compute detail output for a maximum stage water surface profile. The computation setting area of the unsteady flow analysis window contain the computation interval, hydrograph output interval, mapping output interval and detailed output interval (Eichert, 1964). The computation interval is used in the unsteady flow calculation. This is one of the most important parameters entered into the model and selected with care due to it affects the simulation. Firstly, the interval should be small enough too accurately to describe the rise and fall of the hydrograph being routed. In this study it is taken with 20 seconds. In my study 30 minutes is used as hydrograph output interval. The detailed output interval field allows the user to write out profiles of water surface elevation and flow at a user specified interval during the simulation. One hour is used for detailed output interval. For medium to large rivers, the courant condition may yield time steps that are too restrictive (a larger time step could be used and still maintain accuracy and stability). The smaller time step is needed when there is lateral weirs/spillways and hydraulic connections between storage areas and the river system. Computational time step stability and accuracy can be achieved by selecting a time step that satisfies the courant condition. Remember that for Hydraulic models, typical time steps are in the range of 1- 60 seconds due to the very fast flood wave velocities (Eichert, 1964).

$$C = \frac{V\Delta T}{\Delta X} \leq 2 \text{ (with } \alpha \max C = 5) \text{ Or } \Delta T \leq \frac{2\Delta X}{V} \text{ (with } C = 2) \dots \dots \dots (3.28)$$

Where: C=Courant Number;

V= Flood wave velocity (wave celerity)

(m/s);

ΔT =Computation time step(s);

ΔX =Average cell size (ft)

3.6.5. 2D energy equation (Mass Conservation)

The continuity equation and momentum equation are the main scientific basis for unsteady flow analysis. The continuity equation is as follow: (Eichert, 1964)

$$\frac{\partial A}{\partial t} + \frac{\partial Q}{\partial s} - q = 0 \dots\dots\dots (3.29)$$

- Where, A = flow area, m²;
- Q = volume of flow, m³/s;
- q = the lateral inflow per unit length, m²/s;
- t = time variable, s;
- s = spatial distance along the direction of flow, m.

3.6.5.1. Diffusion-Wave equation

And one form of the Diffusion-Wave momentum equation is as follow (Eichert, 1964). $\frac{\partial A}{\partial t} + \frac{\partial QV}{\partial s} + gA \left(\frac{\partial z}{\partial s} + sf \right) = 0 \dots\dots\dots (3.30)$

- Where, V = flow velocity, m/s;
- z = elevation of water surface, m;
- g = gravitational acceleration, m/s²;
- Sf = friction slope.

$$sf = \frac{Q^2 n^2}{R^3 * A^2} \dots\dots\dots (3.31)$$

Where, n = manning’s roughness coefficient; R = hydraulic radius, m

3.7.Flood Hazard map

Flood hazards are multifaceted and encompass various dimensions that need to be considered by flood managers. These dimensions include the where, when, how long-lived, and how much adjustment occurs in relation to flood events. To identify and communicate the potential dangers associated with floods, flood hazard maps are created. These maps take into account the depth

and velocity of floodwaters, as the combined effect of these factors determines the severity of the hazard. Geographic Information System (GIS) software is commonly used to map flood hazards and provide visual representations of the areas at risk. These maps assist in decision-making processes regarding land use, emergency planning, and the allocation of resources for flood management and mitigation efforts.

3.8.Flood vulnerability map

A flood vulnerability map is a spatial representation that depicts the areas at risk of flooding and their corresponding levels of vulnerability. It combines various geographic and socio-economic factors to assess the potential impacts of floods on different areas. In flood vulnerability analysis, it is essential to consider different indicators that provide information about exposure, susceptibility, and resilience. These indicators help assess the potential impact and vulnerability of an area to flood events. The collected data for these indicators are then arranged in increasing order to determine the values for the Vulnerability Index.

- Exposure indicators (X_i) represent the elements or factors present in an area that are at risk of being affected by floods. These can include human settlements, infrastructure, cultural heritage sites, agricultural fields, and other relevant components. The exposure index (I) is obtained based on the functional relationship of these indicators, which can be determined using a specific formula.
- Susceptibility indicators (X_i) reflect the potential of a system or its components to be harmed or negatively impacted by flood events. These indicators consider factors such as fragility, social and economic weaknesses, and unfavorable conditions. The susceptibility index (I) is calculated based on the functional relationship of these indicators, which may involve using a formula specific to the study. Resilience represents the ability of a system or community to adapt, cope with, and recover from flood events. It is a measure of the capacity to absorb and mitigate potential damages caused by floods.
- Resilience indicators are important in understanding the system's ability to withstand and recover from flood impacts.

The vulnerability of a system to flood events can be expressed with the following general equation (Balica, 2007, p 37). This equation is used in the present study to compute Flood Vulnerability Index (FVI).

$$\text{FVI} = \text{Exposure Index} * \text{Susceptibility Index} - \text{Resilience Index} \dots\dots\dots(3.32)$$

. Based on the literatures reviewed, field visit and focused group discussion (FGD) with key informants in the study area, the socio-economic indicators such as, Flood depth, Flood velocity, flood duration, slope, DEM and land-use, are selected in this study as they so much influence the vulnerable nature of the study area.

3.9.Flood Risk Analysis

Flood risk analysis is a process of assessing and evaluating the potential risks associated with flooding in a particular area. For this study, flood hazard and flood vulnerability have been developed, flood risk then developed by overlaying flood hazard map and food vulnerability map. According to Zimmermann, 2005) the conventional expression of risk is,

$$\text{Risk} = \text{Hazard} * \text{Vulnerability} \dots\dots\dots(3.33)$$

4. RESULTS AND DISCUSSION

4.1. HEC-HMS Hydrologic model simulation

The hydrologic simulation of the Waja watershed was conducted using the Hydrologic Engineering Center's Hydrologic Modeling System (HEC-HMS), which is designed to simulate the precipitation-runoff processes within a watershed. This process involved a comprehensive calibration and validation phase to ensure the model's accuracy and reliability. The calibration period spanned from 1996 to 2005, during which various model parameters were precisely adjusted to align the simulated outputs with observed hydrologic data. Following calibration, the validation period from 2006 to 2010 provided an independent assessment of the model's performance. During this phase, the model was tested against a different set of observed data that had not been utilized during calibration. This approach ensured that the model's predictive capabilities were robust and could accurately simulate runoff generation under varying meteorological conditions. The validation results were crucial for confirming the model's reliability, as they indicated how well it could forecast hydrologic responses in the watershed based on new rainfall and land use scenarios.

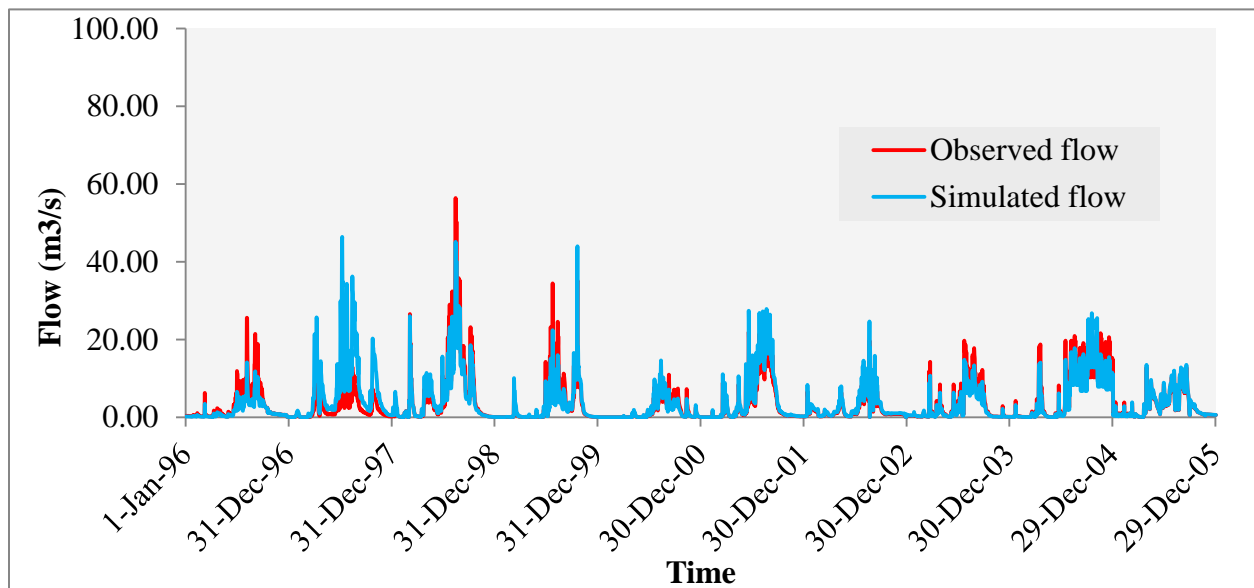
4.1.1. Model Calibration

The analysis of simulated and observed flow values at the outlet of the Waja watershed during the calibration period of 1996 to 2005 demonstrates a high degree of accuracy and alignment between the two datasets, as illustrated in Figure 4.1. The results indicate that the calibrated model effectively captures the hydrologic behavior of the watershed, with the simulated flows closely matching the observed data. A key aspect of this comparison is the synchronization of peak flows within the simulated hydrographs and the observed hydrographs, which further validates the model's capacity to replicate the dynamics of the watershed accurately. To quantitatively evaluate the model's performance, various statistical metrics were computed. As presented in Table 4.1, the Nash-Sutcliffe Efficiency (NSE) gives a value of 0.75, reflecting a relatively good fit between the simulated and observed flow data. This suggests that the model is adept at reproducing stream flow patterns, providing confidence in its predictive capabilities.

Table 4.1: model performance measures during the calibration

Measure	Value	Performance rating
Coefficients of determination (R^2)	0.78	Very good
Nash Sutcliffe coefficients (NSE)	0.75	Very good
Root Mean Square Error (RMSE)	2.03	Very good
Percent Bias	2.02	Very good

Additionally, the Percent Bias (PBIAS) was calculated at 2.02, indicating a slight overall bias in the simulated flows. This suggests that the model may either slightly overestimate or underestimate flows, yet remains within an acceptable range. The coefficient of determination (R^2) was determined to be 0.78, which signifies a reasonably strong correlation between the simulated and observed discharges. This correlation indicates that the model successfully captures a significant portion of the variability present in the observed flow data. Moreover, the Relative Mean Square Error (RMSE), calculated at 2.03, reflects a relatively low level of error in the simulated hydrographs when compared to the observed data. This low error rate reinforces



the reliability of the model in accurately depicting hydrologic conditions within the watershed.

Figure 4.1: Simulated and observed flows during calibration

4.1.2. Model Validation

The validation of the model for the Waja watershed shows its capability to simulate stream flows effectively beyond the calibration period. The validation period, spanning from 2006 to 2010, is illustrated in Figure 4.2, which shows that the simulated and observed stream flow hydrographs exhibit a strong correlation.

Particularly, the peak flows in the simulated hydrographs align closely with those recorded, indicating that the model successfully captures the watershed's dynamics. To quantitatively assess the model's performance during this validation period, several statistical metrics were calculated, as shown in Table 4.2.

The coefficient of determination (R^2) is 0.77, signifying a reasonably strong correlation between simulated and observed discharges. This indicates that the model accounts for a significant portion of the variability in the flow data. Additionally, the Nash-Sutcliffe Efficiency (NSE) value of 0.76 reflects a good fit between the simulated and observed data. The Percent Bias (PBIAS) value of 1.3 suggests a minimal overall bias in the simulated flows.

Furthermore, the Relative Mean Square Error (RMSE) of 1.64 indicates a moderate level of error when comparing the simulated hydrographs to the observed data.

Table 4.2: model performance measures during the validation

Measure	Value	Performance rating
Coefficients of determination (R^2)	0.77	Very good
Nash Sutcliffe coefficients (NSE)	0.76	Very good
Root Mean Square Error (RMSE)	1.3	Very good
Percent Biass	1.64	Very good

Generally, the results of the model validation in the Waja watershed demonstrate a good agreement between the simulated and observed hydrographs during the validation period.

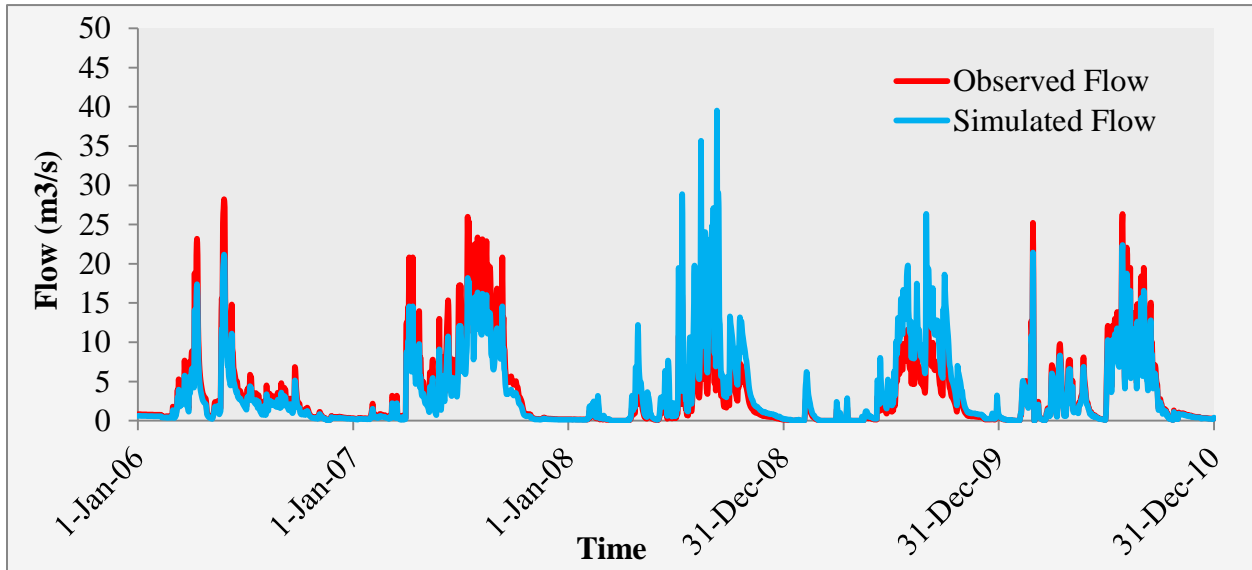


Figure 4.2: Simulated and observed flows during Validation

4.1.3. Peak flood hydrographs

To visualize the variation in flow over time for different storm events of varying frequencies, Figure 4.3 displays the flood hydrographs estimated using the HEC HMS model. These hydrographs represent the simulated flow patterns during different flood events with specific return periods. The figure provides a graphical representation of how the flow changes over time during these events, allowing for a better understanding of the flood behavior in the Waja River. To further analyze and simulate the flood behavior, the flood hydrographs obtained from the HEC HMS model were utilized as upstream boundary conditions in the HECRAS model. HECRAS is widely used hydraulic modeling software that allows for the unsteady simulation of floods and the evaluation of their impacts on river channels and floodplains. By incorporating the HEC HMS-derived flood hydrographs as input, the HECRAS model enables a more detailed examination of flood propagation, channel capacity, and floodplain inundation within the Waja River system. This integrated approach, combining the HEC HMS and HECRAS models, provides a comprehensive analysis of flood behavior in the Waja River. It allows for a better understanding of the flood risk, the potential extent of inundation, and the corresponding impacts on infrastructure, communities, and the environment. Such analyses are crucial for effective

flood management, emergency preparedness, and the development of mitigation strategies in the Waja watershed.

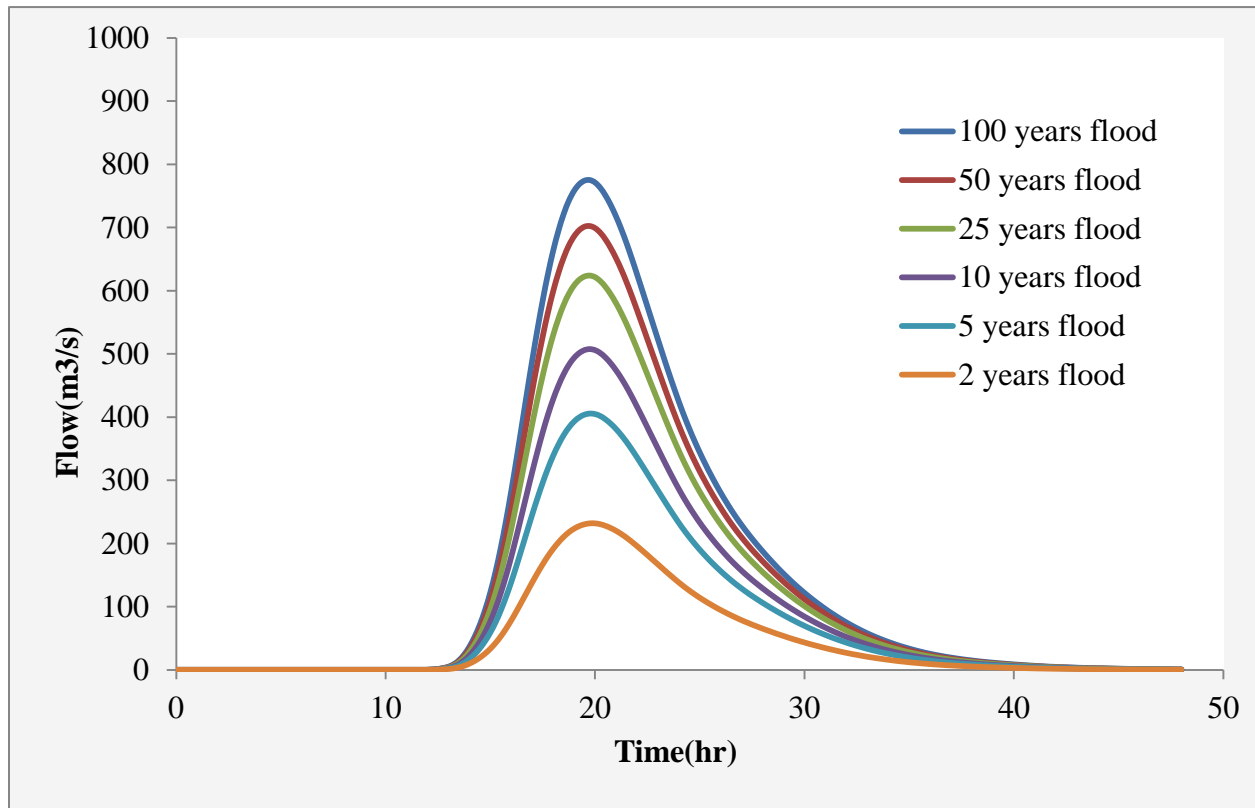


Figure 4.3: Flood hydrograph for different return period

4.2.Flood inundation boundaries

The study aimed to assess the extent of flooding in the Waja River watershed and develop flood inundation maps for different return periods. These maps are essential for emergency response planning and implementing measures during or after flood events. The flood inundation maps indicate the areas that are likely to be affected by floodwaters based on the specified return periods. This information helps stakeholders, such as emergency responders and local communities, understand the potential extent of flooding and take appropriate actions to mitigate its impact. This year, the Waja River floods affected six Kebeles across two districts, displacing over 1,000 households and leaving more than 5,000 residents homeless. The floods also severely impacted local agriculture, submerging more than 1,400 crop fields and displacing over 5,000 livestock. By mapping flood coverage for different flood frequencies, this study offers valuable insights for land use planning, infrastructure development, and emergency preparedness. It

enables authorities to prioritize resources and interventions in the most vulnerable areas, including the implementation of early warning systems, the construction of flood protection structures, and the development of evacuation plans. Table 4.2 below illustrates the flood areal coverage within the study area.

Table 4.3: Flood areal coverage's with corresponding flood frequency

Flood frequency	Areal coverage(ha)
10 years' flood	3030
25 years' flood	3364
50 years' flood	3520
100 years' flood	3683

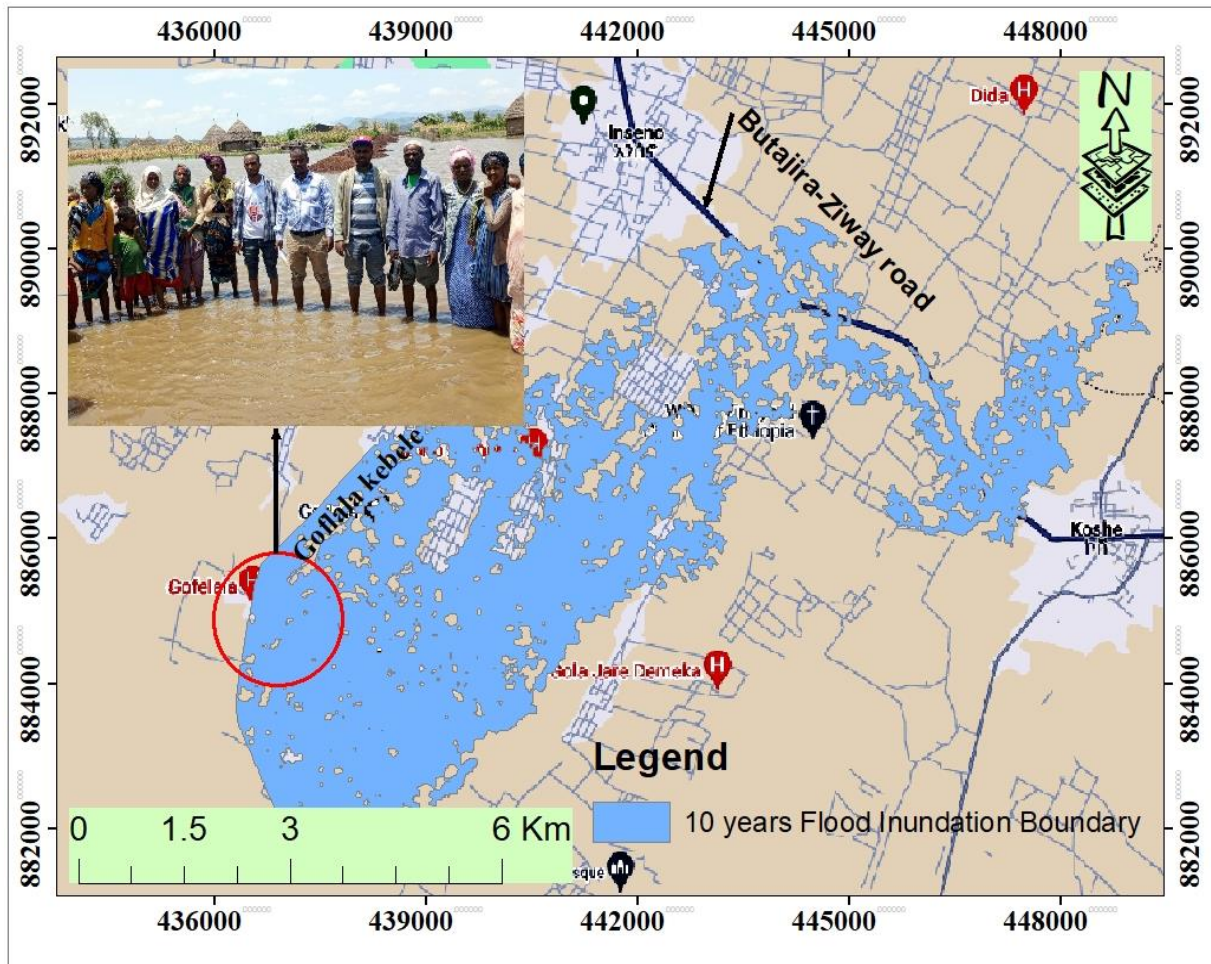


Figure 4.4: River inundation for 10 years storm frequency

4.3.Flood depth

Flood depth information is crucial for assessing flood risk and developing flood hazard maps. These maps provide visual representations of the potential extent of flooding at different water depths, enabling communities and decision-makers to understand the areas prone to flooding and plan accordingly. Flood depth maps are used to identify flood-prone areas, establish floodplain management strategies, and guide land use policies to minimize exposure to flood hazards. Furthermore, flood depth data is essential for infrastructure planning and design. It helps engineers and designers determine the appropriate elevation and flood proofing measures for infrastructure such as buildings, roads, bridges, and drainage systems. In the case of the Waja River flood, the maximum flood depths were found to be 14.45m, 12.6m, 9.2, and 6.3m for return periods of 100, 50, 25, and 10 years, respectively. These depth values indicate the level of floodwater that can be expected at various locations along the river.

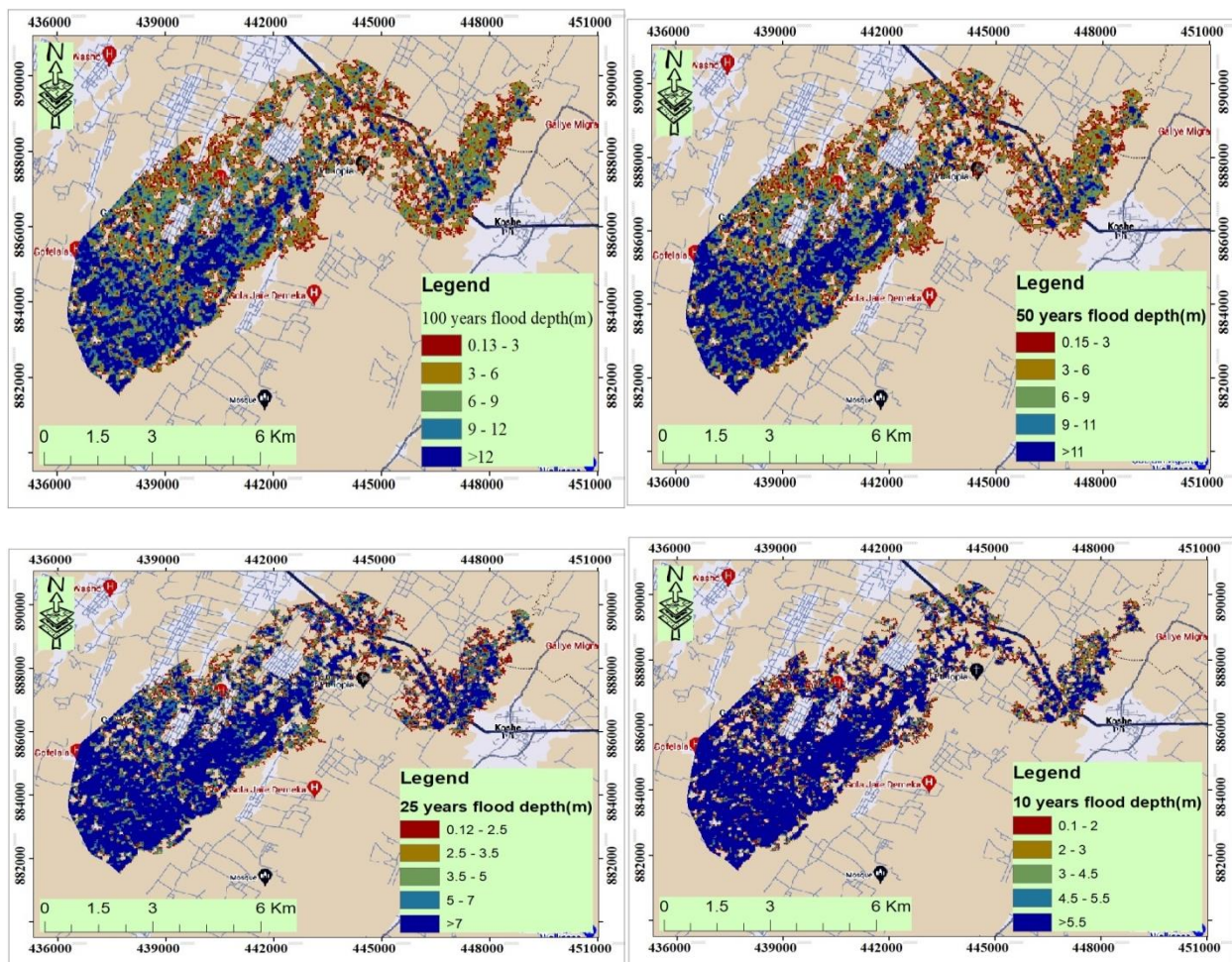


Figure 4.5: Waja river flood depths

By analyzing the flood depth maps, it becomes clear that the maximum flood depth is concentrated in the upstream section of the river channel. This phenomenon can be attributed to the topographical characteristics of the inundated area, which typically features a nearly flat to gently sloping landscape. In these upstream regions, the gradual slope allows for a larger volume of water to accumulate, as the slower gradient reduces the velocity of water flow. Consequently, when heavy rainfall or storm events occur, the water tends to pool more readily in these flatter areas, resulting in increased flood depths. This accumulation is exacerbated by the limited drainage capacity of the surrounding terrain, which can hinder the efficient movement of water downstream

4.4.Flood Velocity

Understanding flood velocity is important for several reasons. First, it helps in assessing the potential risks and hazards associated with flooding. Higher velocities can increase the erosive power of the water, leading to more significant damage to structures, infrastructure, and natural habitats.

Flood velocity also plays a crucial role in determining the effectiveness and design of flood control and mitigation measures. For example, when constructing flood defense structures such as levees or floodwalls, engineers need to consider the anticipated flood velocity to ensure that the structures are designed to withstand the forces exerted by fast-flowing water.

The flood velocity of Waja River was shown on the figure 4.6 below. The result shows that, the maximum flood velocities for 100, 50, 25, 10 years flood frequency are, 6.8, 5.5, 4.7, and 3.8 m/s respectively. The simulation produced variable flow velocities in the main channel and the inundated floodplain. Generally, high velocities were recorded in the main channel than the floodplains.

The spatial distribution of inundation flow velocity demonstrates a clear correlation with the elevation profile of the area. Higher flow velocities are observed at the center of the channel, where the water is deeper and more confined. In contrast, lower velocities are found in the adjacent floodplains, where the terrain is flatter and the water spreads out, reducing its speed.

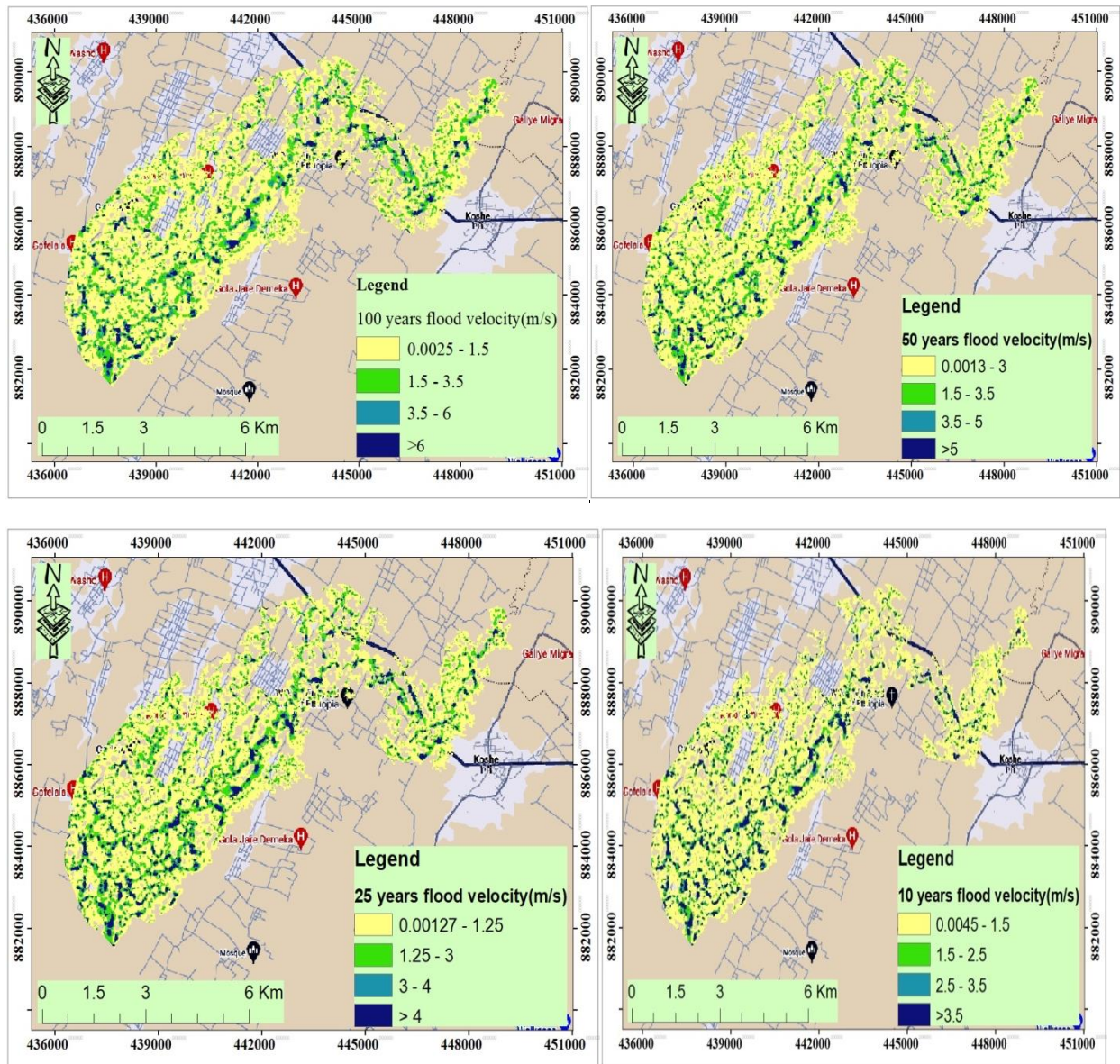


Figure 4.6: Flood velocity of Waja River for different storm frequency

4.5. Flood hazard map

Flood hazard maps incorporate various parameters, including flood extent, flood depth, flood velocity, and duration. Among these factors, flood depth and velocity have the most significant impact on human safety. Flood depth indicates the type of failure that may occur, such as sliding or tumbling failures, while high-velocity floodwaters can directly damage structures or their foundations. As water depth increases, the potential for damage also increases. Higher flood velocities pose a greater risk of loss of life. Even small depths of water moving at high velocities

can cause damage to structures and foundations. Although low-depth, high-velocity flows can cause instability, the chances of drowning are lower compared to deeper water situations, which are more dangerous. Velocities exceeding 2 m/s can result in scouring, affecting the stability of foundations and poles. Erosion of grass and earth surfaces can create scour holes. Depths exceeding 2 m can damage lightly framed buildings through water pressure, floatation, and debris impact, even at low velocities. Therefore, it is essential to consider a comprehensive set of hazard vulnerabilities for classifying flood hazards on a floodplain.

The relative vulnerability of the community and its built assets to flood hazard can be assessed by using flood velocity and depth thresholds. The thresholds are related to the stability of both people and vehicles in flood waters, and to buildings affected by flooding.

For analyzing Waja river flood hazard classification, the combined effect of flood depth and velocity has been considered. These hazard criteria are assigned hazard index on 1 – 5 scale, 1 being low hazard category while 5 being extreme hazard category. The hazard classification scheme developed by FEMA (2018) is shown in table 4.4 below.

Table 4.4:Flood Depth and Velocity Severity Grid Categories source: FEMA (2018)

Flood index	Flood severity category	Depth *velocity range (m ² /sec)	Description
1	Low hazard	≤ 0.2	Generally safe for vehicles, people and buildings.
2	Medium hazard	0.2 - 0.5	Unsafe for small vehicles.
3	High hazard	0.5 - 1.5	Unsafe for vehicles, children and elderly.
4	Very high hazard	1.5 - 2.5	Unsafe for vehicles and peoples
5	Extreme hazard	> 2.5	Unsafe for all vehicles, peoples, and buildings

The flood hazard map created for the Waja River floodplain, considering a 100-year return period, has provided valuable insights. The results indicate that a significant portion, approximately 35%, of the flooded area falls under the categories of Extreme, very high and high hazard. These hazardous zones predominantly encompass the rural settlements of six Kebeles across two districts of Silte zone and the agricultural lands located within the floodplain.

Furthermore, the flood hazard map reveals that approximately 65% (Table 4.5) of the flooded area is classified as medium and low hazard. These areas are characterized by relatively flat slopes, which may contribute to reduced flood risks compared to the higher hazard zones. However, it is important to note that even within the medium and low hazard areas, precautionary measures and flood preparedness should still be implemented, as flooding can still pose significant challenges and potential damage. The findings of the flood hazard map emphasize the critical importance of understanding and addressing the specific risks and vulnerabilities posed by flooding in the Waja River floodplain. This information can guide decision-makers, urban planners, and emergency management authorities in developing appropriate flood mitigation strategies, land-use planning regulations, and emergency response plans to safeguard the affected communities and minimize the potential impacts of future flood events.

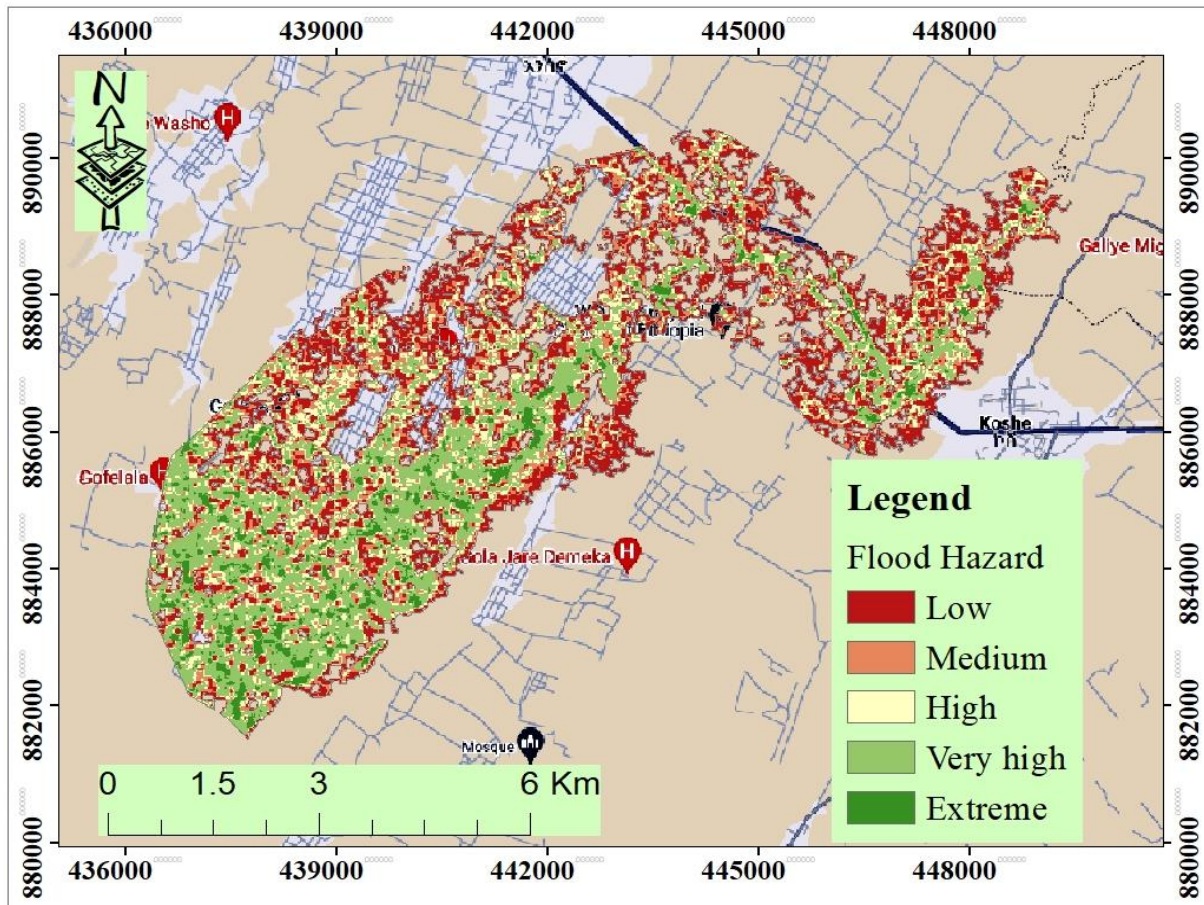


Figure 4.7: Flood hazard classes of 100 year flood

Table 4.5: Flood hazard coverage of Waja River

Hazard class	Area(ha)	Inundation coverage (%)
Low	1243	34%
Medium	1157	31%
High	675	18%
Very high	498	14%
Extreme	110	3%

4.6.Flood Vulnerability Map

When developing a flood vulnerability map, several parameters are typically considered. By integrating and analyzing those factors, a flood vulnerability map assigns varying levels of vulnerability to different areas or communities. The flood vulnerability map specifically designed for the Waja River floodplain, with a focus on the 100-year return period, has yielded significant insights into the area's vulnerability to flooding. The map has effectively identified and classified different vulnerability levels across the region, providing valuable information for decision-making and flood risk management.

According to the flood vulnerability map shown on figure 4.8 above and table 4.6 below, approximately 17% of the flooded area is categorized as having high and very high vulnerability. These areas primarily consist of the rural Kebeles' of Silte Kebeles. The concentration of high vulnerability in this region indicates an increased risk of flooding and highlights the urgent need for proactive measures to mitigate the impacts on the population and infrastructure. Around 18% of the flooded area falls under the moderate vulnerability class. The majority of the flooded area, covering approximately 65%, is classified as having low and very low vulnerability. These areas predominantly consist of vegetation, and grasslands. While these regions are considered less vulnerable to flooding, it is crucial to maintain awareness and preparedness, as even low vulnerability areas can be affected by extreme flooding events.

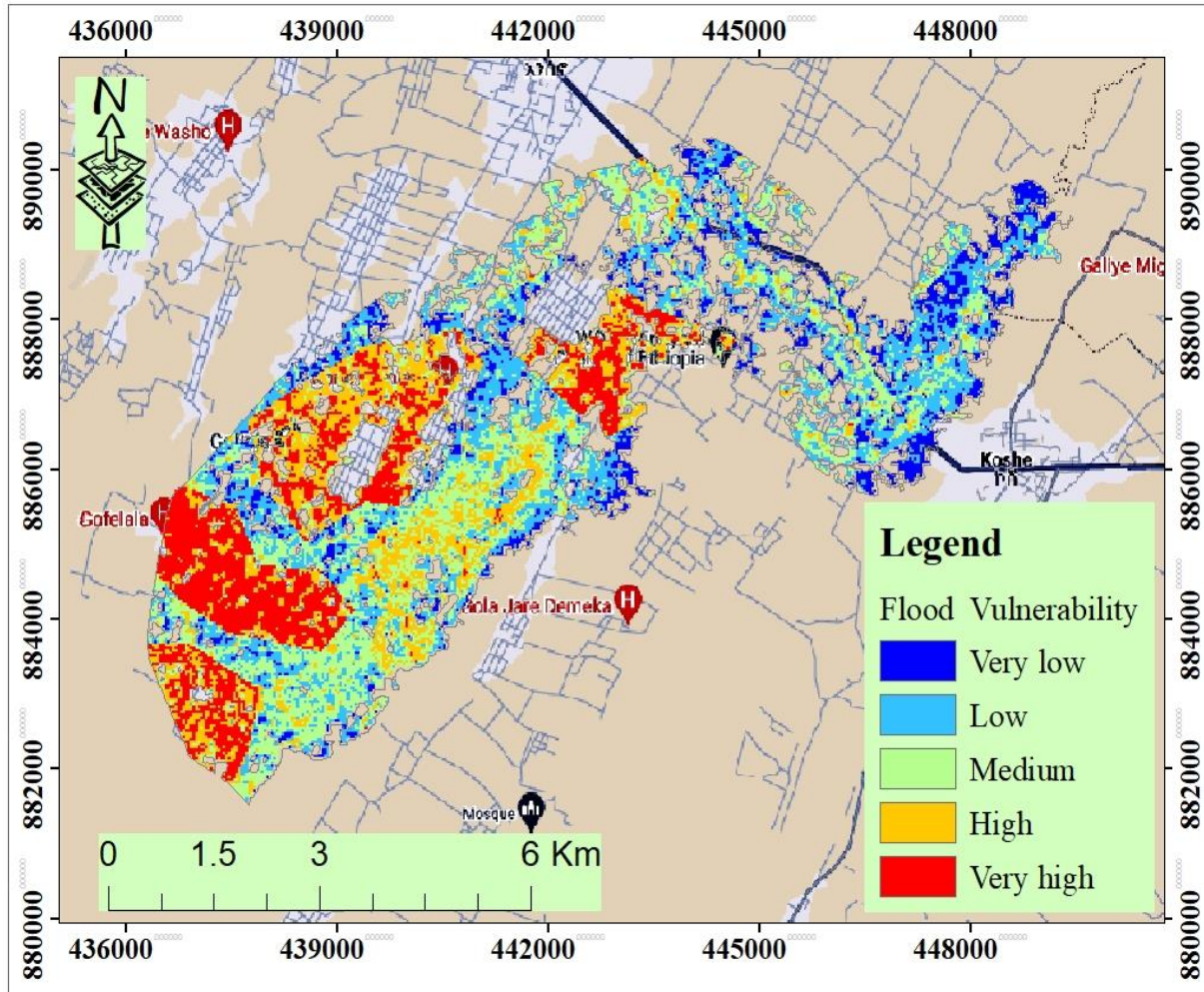


Figure 4.8: Flood vulnerability map of Waja River floodplain

Table 4.6: Flood Vulnerability coverage of Waja River

Vulnerability Level	Area(ha)	Coverage (%)
Very low	1243	34%
Low	1157	31%
Moderate	675	18%
High	498	14%
Very high	110	3%

4.7.Flood Risk Map

A flood risk map is a geographical representation that assesses and illustrates the potential risks associated with flooding in a particular area. It combines various factors, such as flood hazards and vulnerability to provide a comprehensive understanding of the overall flood risk in a region. By integrating these factors, a flood risk map assigns varying levels of risk to different areas within a region. Typically, risk levels are categorized as high, moderate, or low, based on the combined assessment of hazards and vulnerability. The map provides a visual representation of the areas that are most at risk, allowing stakeholders to make informed decisions regarding land use planning, emergency response, and long-term flood risk management strategies. A comprehensive flood risk map serves as a valuable tool for policymakers, urban planners, emergency management agencies, and communities. It helps identify areas that require immediate attention and investment in flood mitigation measures. By understanding the specific risks and vulnerabilities associated with flooding, stakeholders can develop appropriate strategies to reduce the impact of flood events, enhance community resilience, and protect lives and property.

The flood risk map of the Waja River floodplain provides a comprehensive understanding of the flood risk levels across the region. The map classifies the flood risk into five levels, ranging from very low to very high risk, based on an analysis of various factors including hazards and vulnerability. According to table 4.7 below, the flood risk map, approximately 24% of the flooded area falls under the category of very high and high risk. These areas are predominantly characterized by the six rural Kebeles particularly Goflala kebele was the most risky area. The concentration of very high and high-risk zones in those Kebeles underscores the significant vulnerability of these areas to flooding. It highlights the urgent need for effective flood mitigation measures, emergency response plans, and infrastructure improvements to protect the lives and properties of the residents. Approximately 45% of the flooded area is classified as low and very low risk. These regions are primarily located downstream which are sparse rural populations and natural vegetation. Around 20% of the flooded area is categorized as moderate risk. In general the flood risk map provides valuable information for policymakers, urban planners, and emergency management authorities to prioritize resources and implement appropriate measures. By understanding the specific areas and communities at different levels of

flood risk, stakeholders can develop tailored strategies for flood risk reduction, land-use planning, and emergency response. This includes implementing protective infrastructure, improving early warning systems, and promoting community engagement and education initiatives.

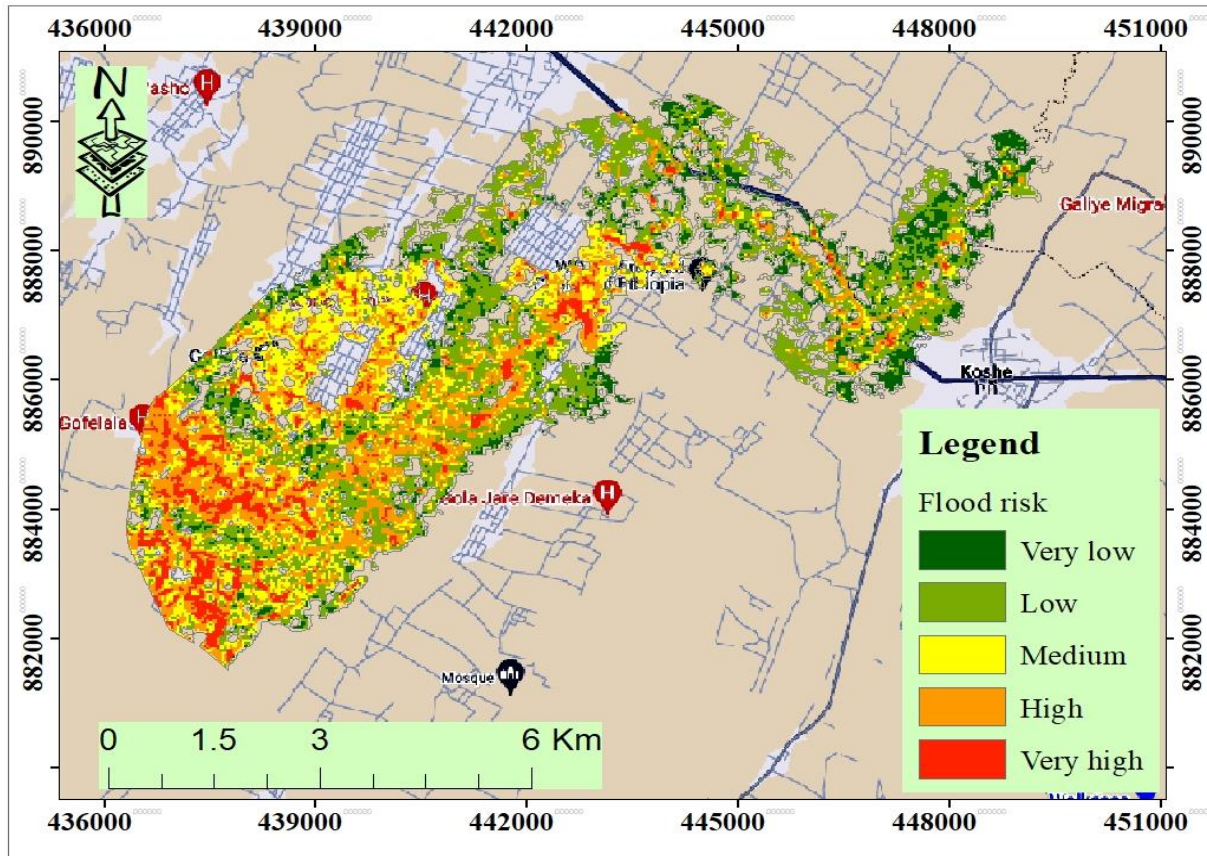


Figure 4.9: Flood risk map of Waja River floodplain

Table 4.7: Flood Risk coverage of Waja River

Risk Level	Area(ha)	Coverage (%)
Very low	454.6	12%
Low	1233.6	33%
Moderate	725.6	20%
High	891.6	24%
Very high	377.6	10%

5. CONCLUSION AND RECOMMENDATION

5.1. Conclusion

The study was conducted on the Waja River floodplain aimed to model and maps the flood hazard, vulnerability, and risk associated with flooding in the area. To achieve this objective, various data sources were utilized, including meteorological, hydrologic, and topographic data collected from different organizations. Meteorological data was obtained from the National Meteorological Agency (NMA), stream flow data from the Hydrology Department of the Ministry of Water and Energy (MoWE), and topographic data from high-resolution Digital Elevation Models (DEM) downloaded from the Alaska Satellite Facility. The study employed several tools and materials, including the HEC HMS (Hydrologic Engineering Center Hydrologic Modeling System) and HEC-RAS (Hydrologic Engineering Center's River Analysis System) models, GIS software, GPS devices, and metering tape. The HEC HMS model was used to analyze flood hazard and risk by developing inflow design floods for different return periods based on daily rainfall and observed stream flow data. The model was calibrated and validated using actual stream flow data, demonstrating a strong relationship between simulated and observed data as indicated by the statistical metrics calculated during the calibration and validation periods. Accordingly, during model calibration the NSE value was 0.75, Percent Bias (PBIAS) was 2.02, coefficient of determination (R^2) was 0.78, and Relative Mean Square Error (RMSE) was 2.03, indicating a good fit, favorable bias, strong correlation, and low error between the simulated and observed flow values. Similarly, during the validation, the model achieved a solid performance with an R^2 of 0.77, NSE of 0.76, PBIAS of 1.64, and RMSE of 1.3, indicating a reasonable fit, slight bias, significant correlation, and acceptable accuracy. These results confirm the model's ability to accurately simulate stream flows and provide valuable insights for hydrologic analysis in the Waja watershed. After calibration and validation, the annual maximum precipitation was extracted from rainfall data to develop frequency storms for different return periods. These storms were then used as input for the HEC HMS model to generate flood hydrographs. The HEC-RAS model, combined with the flood hydrographs, was used to produce flood inundation maps, which were visualized in ARC-GIS software for detailed analysis. The results of the study indicated that for return periods of 10, 25, 50, and 100 years, the areas inundated by floods were 3030 ha, 3364 ha, 3520 ha, and 3683 ha, respectively. Additionally, the maximum flood depths were found to be 6.3m, 9.2m, 12.6m, and 14.45m for the respective

return periods. The maximum flood velocities were 3.8 m/s, 4.7 m/s, 5.5 m/s, and 6.8 m/s for the same return periods.

Flood hazard maps were developed from the depth, velocity, and duration of floodwaters, revealing that 35% of the flooded area falls under the categories of Extreme, very high and high hazard, while approximately 65% was classified as medium and low hazard. The flood vulnerability map, which considered indicators such as flood depth, velocity, duration, slope, land use/land cover, slope and DEM, classified approximately 17% of the flooded area as having high and very high vulnerability. Around 18% of the flooded area falls under the moderate vulnerability class and the majority of the flooded area, covering approximately 65%, is classified as having low and very low vulnerability. By combining the flood hazard and vulnerability information, the study developed a flood risk map, which categorized the risk into five levels: very low, low, medium, high, and very high. The results showed that 24% of the area fell into the high and very high-risk categories. About 20% of the area had a moderate risk and the remaining 45% of the flooded area was classified as low and very low risk.

5.2.Recommendation

Based on the findings of this research, several recommendations can be made to address the risks and vulnerabilities associated with flooding in the Waja River floodplain. These recommendations aim to enhance flood mitigation, improve emergency response, and ensure the safety and resilience of the affected communities:

- **Enhanced Data Collection and Monitoring:** Establish a comprehensive network for real-time meteorological and hydrological data collection. This should include additional rainfall gauges and stream flow monitoring stations to improve data accuracy and model calibration.
- **Regular Model Updates:** Periodically update the HEC HMS and HEC-RAS models with new data to ensure their accuracy over time. Incorporating recent flood events and changing land use patterns will help maintain the models' relevance.
- **Community Engagement and Awareness:** Implement community outreach programs to educate local populations about flood risks and preparedness. Enhancing public awareness can promote better risk management practices among residents in vulnerable areas.

- **Land Use Planning:** Integrate flood risk assessments into land use planning and zoning regulations. Limiting development in high-risk areas can reduce vulnerability and improve community resilience against flooding.
- **Emergency Response Planning:** Develop and regularly update emergency response plans that incorporate flood risk maps. This will aid in efficient evacuation and resource allocation during flood events.
- **Collaboration with Local Authorities:** Foster partnerships with local governments and relevant organizations to facilitate coordinated flood risk management strategies. Collaborative efforts can enhance resource sharing and implementation of effective flood mitigation measures.
- **Future Research:** Encourage further research into climate change impacts on hydrology and flooding patterns in the Waja River floodplain. Understanding these dynamics can inform long-term adaptation strategies.

6. REFERENCES

- Anees, M.T.; Abdullah, K.; Nawawi, M.N.M.; Ab Rahman, N.N.N.; Piah, A.R.M.; Zakaria, N.A.; Syakir, M.I.; Omar, M. 124, 478–486. (2016). *Numerical modeling techniques for flood analysis*. African Earth Sci.
- (Camp, 2. (2001). *Camp, W. G. (2001). Formulating and Evaluating Theoretical Frameworks for Career and Technical Education Research. Journal of Vocational Educational Research, 26, 27-39.*
- (Shustikova et al. . (2019). Comparing 2D capabilities of HEC-RAS and LISFLOOD-FP on complex topography. *Hydrological Sciences Journal/Journal des Sciences Hydrologiques* , 64(14).
- Abera, Z. (2011). *Flood Mapping and Modeling on Fogera Flood Plain: A Case Study of Ribb River*. Ethiopia.
- Abu, K. (2020). *Flood Risk Mapping (Case Study of Ketar Watershed Ziway-Dugda Woreda, Ethiopia*. ADDIS ABABA.
- Adhanom, N. a. (2019). *Flood Hazard and Flood Risk Vulnerability Mapping Using Geo Spatial and MCDA around Adigrat*,. Tigray.
- Ahmad SS, Simonovic SP . (2013). Spatial and temporal analysis of urban flood risk assessment. *Urban Water J*.
- Akawka & Haile, 2. (2021). Implications of water abstraction on the interconnected Central Rift Valley Lakes sub-basin of Ethiopia using WEAP.
- ALEMAYEHU, D. (2007). *ASSESSMENT OF FLOOD RISK IN DIRE DAWA TOWN, EASTERN ETHIOPIA, USING GIS*. ADDIS ABABA.
- Alemu, Y. T. (2015). Flash Flood Hazard in Dire Dawa, Ethiopia. *Journal of Social Sciences and Humanities*.

- Amrei David,& Britta Schmalz. (2020). Flood hazard analysis in small catchments: Comparison of hydrological and hydrodynamic approaches by the use of direct rainfall. *Flood Risk Management*.
- Anbessie, A. S. (2023). *A Thesis Submitted to Hawassa University School of Graduate Studies* in. aa: xz\ssd.
- Anees, M.T & et al. (2016). Numerical modeling techniques for flood analysis. *African Earth Sci.*, 124, 478–486.
- Anees, M.T. (n.d.).
- Anees, M.T.; Abdullah, K.; Nawawi, M.N.M.; Ab Rahman, N.N.N.; Piah, A.R.M.; Zakaria, N.A.; Syakir, M.I.; Omar, M. J. (2016.). Numerical modeling techniques for flood analysis. 124, 478–486.
- Belina, Y. (2020). *“Flood Mapping and Mitigation Measures for Upper Awash River”*.
- Bengtson, M. L. (1999). *A HYDROLOGIC MODEL FOR ASSESSING THE INFLUENCE OF WETLANDS ON FLOOD HYDROGRAPHS IN THE RED RIVER BASIN DEVELOPMENT AND APPLICATION*. North Dakota: International Joint Commission Red River Task Force North Dakota State Water Commission.
- Bhagat, N. (2017). Flood Frequency Analysis Using Gumbel's Distribution Method: A Case Study of Lower Mahi Basin, India. *Ocean Development and International Law* 6(4):51-54.
- Brilly, M. (2005). *Public perception of flood risks, flood forecasting and mitigation*. Natural Hazards and Earth System Sciences.
- Bronstert, A. (2003). *Floods and Climate Change: Interactions and Impacts*. *Risk Analysis*.

- Cameron. (2010). *GEOSPATIAL CAPABILITIES OF HEC-RAS FOR MODEL DEVELOPMENT AND MAPPING*. U.S: 2nd Joint Federal Interagency Conference, Las Vegas.
- Camp, J. (2022). *the conversation US* .
- Camp, W. G. (2001). *Formulating and Evaluating Theoretical Frameworks for Career and Technical Education Research. Journal of Vocational Educational Research,*.
- Camp, W. G. (n.d.). *Formulating and Evaluating Theoretical Frameworks for Career and Technical Education Research. Journal of Vocational Educational Research.*
- Cançado, V. (2010). *Economical consequences of floods: modelling impacts in urban areas* . Poland: Fifth SWITCH Scientific Meeting, Lodz.
- Cedillo, P. E. (2015). Hydrodynamic Modeling of the Green Bay of Lake Michigan Using the Environmental Fluid Dynamics Code. *M.S. thesis, Univ. of Wisconsin-Milwaukee, Milwaukee.*
- Central Water Commission. (2020). New Delehi.
- Chow, V. T. (1988). *Applied Hydrology*. New york.
- Chuanhai Wang et al., (2021). Distributed-Framework Basin Modeling System: I. Overview and Model Coupling. *Modelling Hydrologic Response of Non-homogeneous Catchments.*
- Debarati. (2006). *Socioeconomic Impacts of the 2006 Seasonal Flooding along Flood Prone Areas: The Case of Dire Dawa Administration, Ethiopia.*
- Dilip Kumar and Rajib Kumar Bhattacharjya. (2020). Review of different methods and techniques used for flood vulnerability.
- Dottori et al., 2. (2018). *Increased human and economic losses from river flooding with anthropogenic warming. Nat. Clim. Change,*.

- Fahad, M.G.R. et al. . (2020). Coupled Hydrodynamic and Geospatial Model for Assessing Resiliency of Coastal Structures under Extreme Storm Scenarios. *Water Resources Management* .
- G.Venkata Bapalu, R. S. (2014). *GIS in Flood Hazard Mapping: a case study of Kosi River Basin, India*. India: Rajiv Sinha on 09 July 2014.
- Garcia-Alen et al. . (2023). Comprehensive Overview of Flood Modeling Approaches: A. *Hydrology*.
- Gebre, G. a. (2015). Flood Hazard Assessment and Mapping of Flood Inundation Area of the Awash River Basin in Ethiopia using GIS and HEC-GeoRAS/HEC-RAS Model. *Journal of Civil & Environmental Engineering*.
- Gebre, Yitea Seneshaw Getahun and Sintayehu Legesse. (2015). Flood Hazard Assessment and Mapping of Flood Inundation Area of the Awash River Basin in Ethiopia using GIS and HEC-GeoRAS/HEC-RAS Model,. *J. Civ. Environ. Eng.,vol. 05, no. 04.*.
- GELBURD, D. (2021). HEC-RAS 6.0 Computer Program and Documentation.
- Gunathilake, M. B. (2019). Application of HEC-HMS model to simulate long term streamflow in the Kelani River Basin, Sri Lanka.
- Hagos, B. (2011). *Hydraulic Modeling and Flood Mapping Of Fogera Flood Plain: A Case Study of Gumera River*. Addis Ababa.
- Hongren Shen,& Bryan A. Tolson. (2022). Time to Update the Split-Sample Approach in Hydrological Model Calibration.
- Imenda, S. (. (2014). *Is There a Conceptual Difference between Theoretical and Conceptual Frameworks? Journal of Social Sciences, 38, 185-195.*

- Jahandideh-Tehrani et al., (2021). *Calibration of conceptual rainfall-runoff models by selected differential evolution and particle swarm optimization variants.*
- Jayaseelan, A. (2001). *Droughts and Floods Assessment and Monitoring Using Remote Sensing .*
India: Satellite Remote Sensing and GIS Applications in Agricultural Meteorology.
Department of Space, Govt. of India,.
- Jonkman. (2005). *Global Perspectives on Loss of Human Life Caused by Floods.*
- Kemal, Chekole Tamalew & Abdella. (2016). Estimation of Discharge for Ungauged Catchments Using Rainfall-runoff Model in Didessa Sub-basin: the Case of Blue Nile River Basin, Ethiopia.
- Khan and Rahman. (2015). *A review and future directions of brand experience research.*
- Lu. Marinah Muhammad & Zudi, . (2020). Estimating the UK Index Flood: an Improved Spatial Flooding Analysis. *Estimating the UK Index Flood: an Improved Spatial Flooding Analysis.*
- Luse, M. e. (2012). *Selecting a Research Topic:A Framework for Doctoral Students Iowa State University, Ames, IA, USA.*
- M. I. Zafar. (2021). *IMPROVING FLOOD ESTIMATION IN UNGAUGED.* University of Bristol, Bristol, U.K.
- Manfreda, S. (2008). *FLOOD VOLUME ESTIMATION AND FLOOD MITIGATION: ADIGE RIVER BASIN.* Italia : E. Wiegandt (ed.), Mountains: Sources of Water, Sources of Knowledge.
- Mark Velasquez & Patrick Thomas Hester. (2013). An Analysis of Multi-Criteria Decision Making Methods . *nternational Journal of Operations Research Vol. 10, No. 2, 56–66 .*

- Marsooli, R.; et al. (2021). Climate Change Impacts on Wind Waves Generated by Major Tropical Cyclones off the Coast of New Jersey, USA.
- Merwade, V. (2016). *Tutorial on using HEC-GeoRAS with ArcGIS 10.x and HECRAS Modeling*. School of Civil Engineering, Purdue University.
- Mishra et al. (2022). *Land use change and carbon emissions of a transformation to timber cities*.
- Mokonen, D. (2021). *FLOOD RISK ANALYSIS (Case Study of Upper Awash River from*. Addis Ababa.
- Mulu, H. D. (2021). Mapping flood inundation areas using GIS and HEC-RAS model at Fetam River, Upper Abbay Basin, Ethiopia. *Scientific African*.
- Namara, W. G. (2020). RAINFALL RUNOFF MODELING USING HEC-HMS:THE CASE OF AWASH BELLO SUB-CATCHMENT, UPPER AWASH BASIN, ETHIOPIA. *INTERNATIONAL JOURNAL OF ENVIRONMENT*, Volume-9, Issue-1, 2019/20.
- Negash, M. (2014). *Farmers' adoption of soil and water conservation technology: a case study of the Bokole and Toni sub-watersheds, southern Ethiopia*.
- NMA. (2018). *Revised Flood Alert*. Addis Ababa: Early Warning and Emergency Response Directorate.
- Peshkin, A. (. (1993). *The goodness of qualitative research*.*Educational Researcher*, 22(2), 23-29.
- Pontes, P.R.M.; Fan, et al, . (2022). Effects of Climate Change on Hydrology in the Most Relevant Mining Basin in the Eastern Legal Amazon.
- Rahman, (. a. (2015). *A review and future directions of brand experience research*.
- Ronghua Liu et al, . (2022). Model integration methods for hydro-model platform under cloud computing environments. *Frontiers in Environmental Science*.

- Roy, S.K. and Sarker, S.C. (2016). Integration of Remote Sensing Data and GIS Tools for Accurate Mapping of Flooded Area of Kurigram. *Journal of Geographic Information System*, 8, 184-192.
- Saaty, T. (2008). Decision Making with the Analytic Hierarchy Process. *International Journal of Services Sciences*, 1, 83.
- SALHAIN, JUN RENTSCHLER & MELDA. (2020). *Developmental and Climate change*. World Bank.
- Sandeep Samantaray & Abinash Sahoo. (2020). Estimation of flood frequency using statistical method: Mahanadi River basin, India. *H2Open Journal (2020) 3 (1): 189–207*.
- Sarra Aloui et al. (2023). *A review of Soil and Water Assessment Tool (SWAT) studies of Mediterranean catchments: Applications, feasibility, and future directions*.
- Schubert et al. (2023). Comprehensive Overview of Flood Modeling Approaches: A Review of Recent Advances. *Hydrology* .
- Setegn. (2010). *Modelling Hydrological and Hydrodynamic Processes in Lake Tana Basin, Ethiopia*.
- Sherly et al.,. (2015). Design Rainfall Framework Using Multivariate Parametric-Nonparametric Approach. *journal of hydrology*.
- Shuai Xie et al. (2021). Artificial neural network based hybrid modeling approach for flood inundation modeling. *Journal of Hydrology*.
- Simons, G.& et al. (2016). Integrating global satellite-derived data products as a pre-analysis for hydrological modelling studies: A case study for the red river basin. *Remote Sens*. 8, 279.
- Singh et al.,. (2020). *flood prone areas by an integrated framework of a hydrodynamic model and ANN*.

- Singh, Mohita Anand Sharma & J.B. Singh. (2010). Use of probability distribution in rainfall analysis. *Statistical Analysis*.
- Sinha, R. (2005). *GIS in Flood Hazard Mapping: a case study of Kosi River Basin, India*. India: See discussions, stats, and author profiles for this publication .
- Sisay, D. (2015). *Flood Risk Analysis in Illu Floodplain, Upper Awash River Basin, Ethiopia*. ADDIS ABABA.
- Subramanya, K. (. (2009). *Flow In Open Channels. 3rd Edition*, . New Delhi: Tata Mc Grow-Hill,.
- Subramanya, K. (2008). *Engineering Hydrology. 3rd Edition, Tata McGraw-Hill Publishing Company Limited, New Delhi*. New Delhi: Scientific Research Publishing Inc.
- Subramanya, K. (2009). *Flow In Open Channels. 3rd Edition*,. New Delhi: Tata Mc Grow-Hill,.
- Tadesse, A. (2017). Prediction of Stream Flow at Ungauged Catchments Using Rainfall-Runoff Model: The Case of Upper Tekeze Basin, Ethiopia.
- Tansar, H. et al,. (2020). Flood inundation modeling and hazard assessment in Lower Ping River Basin using MIKE FLOOD. *Arabian Journal of Geosciences*.
- Tekle, S. (2020). *CLIMATE CHANGE AND INSURANCE INDUSTRY IN ETHIOPIA: CHALLENGES AND OPPORTUNITIES*. Addis Ababa.
- UNICEF. (2022). *Ethiopia Humanitarian Situation Report No. 8*. UNICEF 2022 Ethiopia Humanitarian Action for Children (HAC) Appeal.
- UNOCHA, 2. (2022). *Gambella Region Flood Update*.
- Varshney, P. (2020). *Q-Q Plots Explained, "Understanding the concept of Q-Q plots"*.
- Xiang, Z. (2020). A Rainfall-Runoff Model With LSTM-Based Sequence-to-Sequence Learning. *Water Resources Research* .

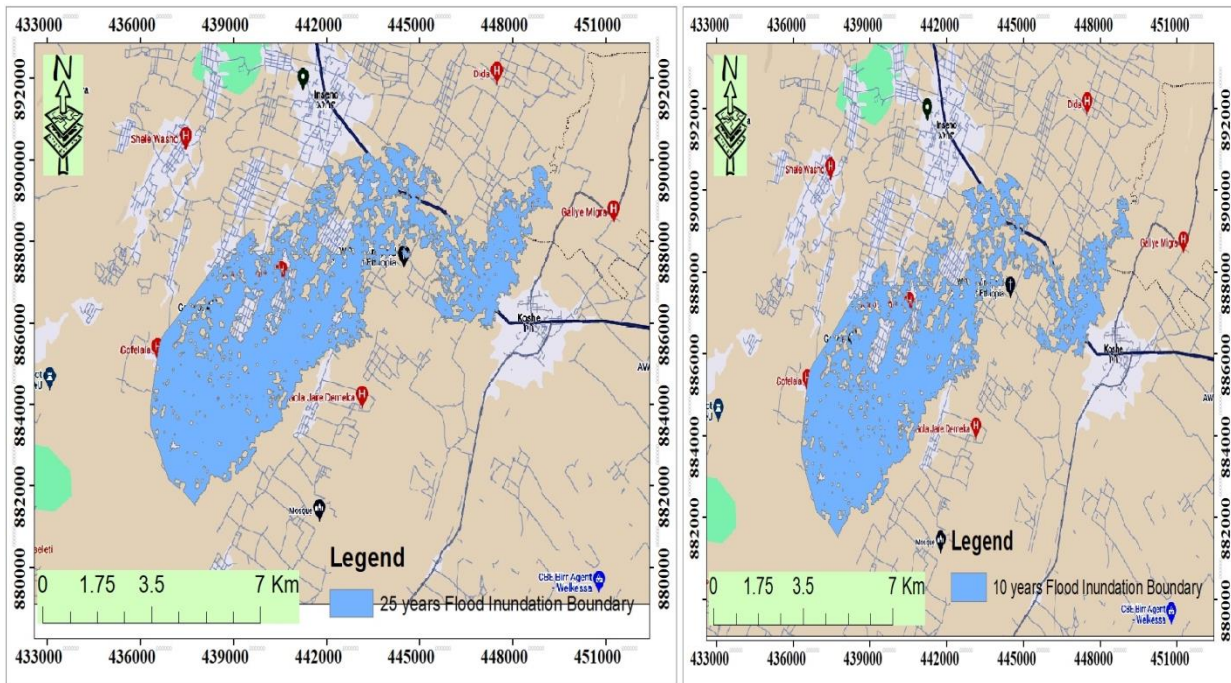
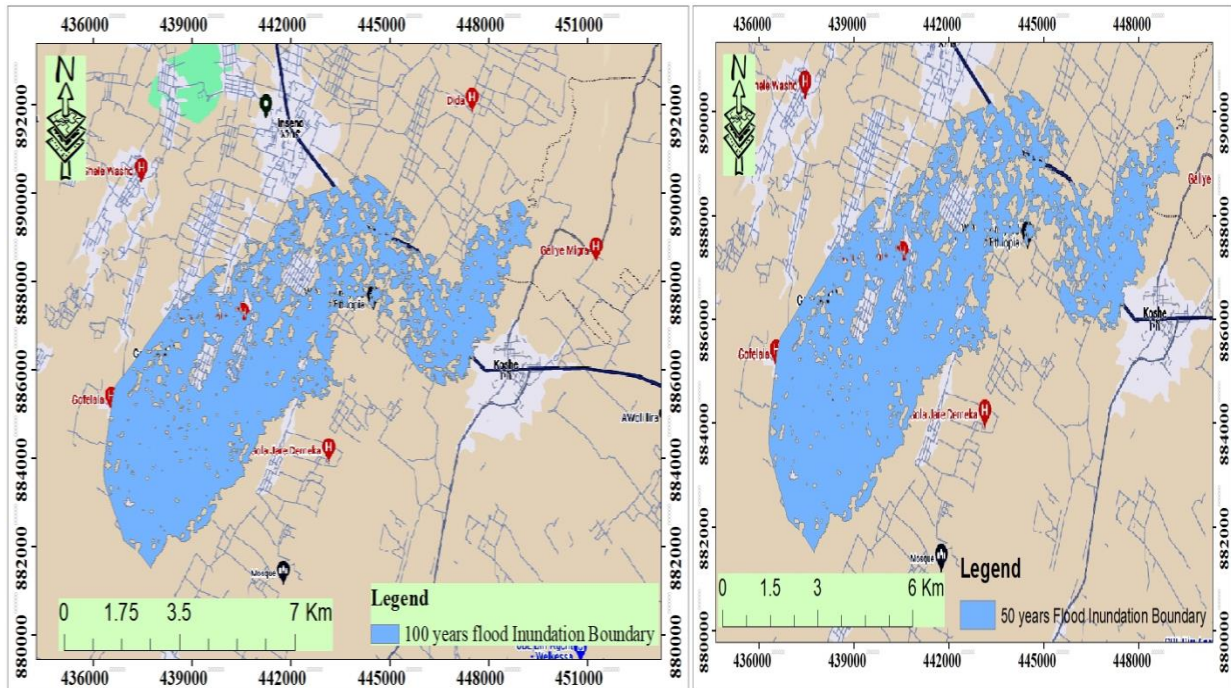
- Xin Jin and Yanxiang Jin . (2020). Calibration of a Distributed Hydrological Model in a Data-Scarce Basin Based on GLEAM Datasets. *Advanced Hydrologic Modeling in Watershed-Scale*.
- Yeshmebet Yitbarek Belay, et al. (2022). Comparison of HEC-HMS hydrologic model for estimation of runoff computation techniques as a design input: case of Middle Awash multi-purpose dam, Ethiopia.
- Zein, M. (2010). *A COMMUNITY-BASED APPROACH TO FLOOD HAZARD AND VULNERABILITY ASSESSMENT IN FLOOD PRONE AREAS*. Indonesia: INTERNATIONAL INSTITUTE FOR GEO-INFORMATION SCIENCE AND EARTH OBSERVATION.

7. ANNEXES

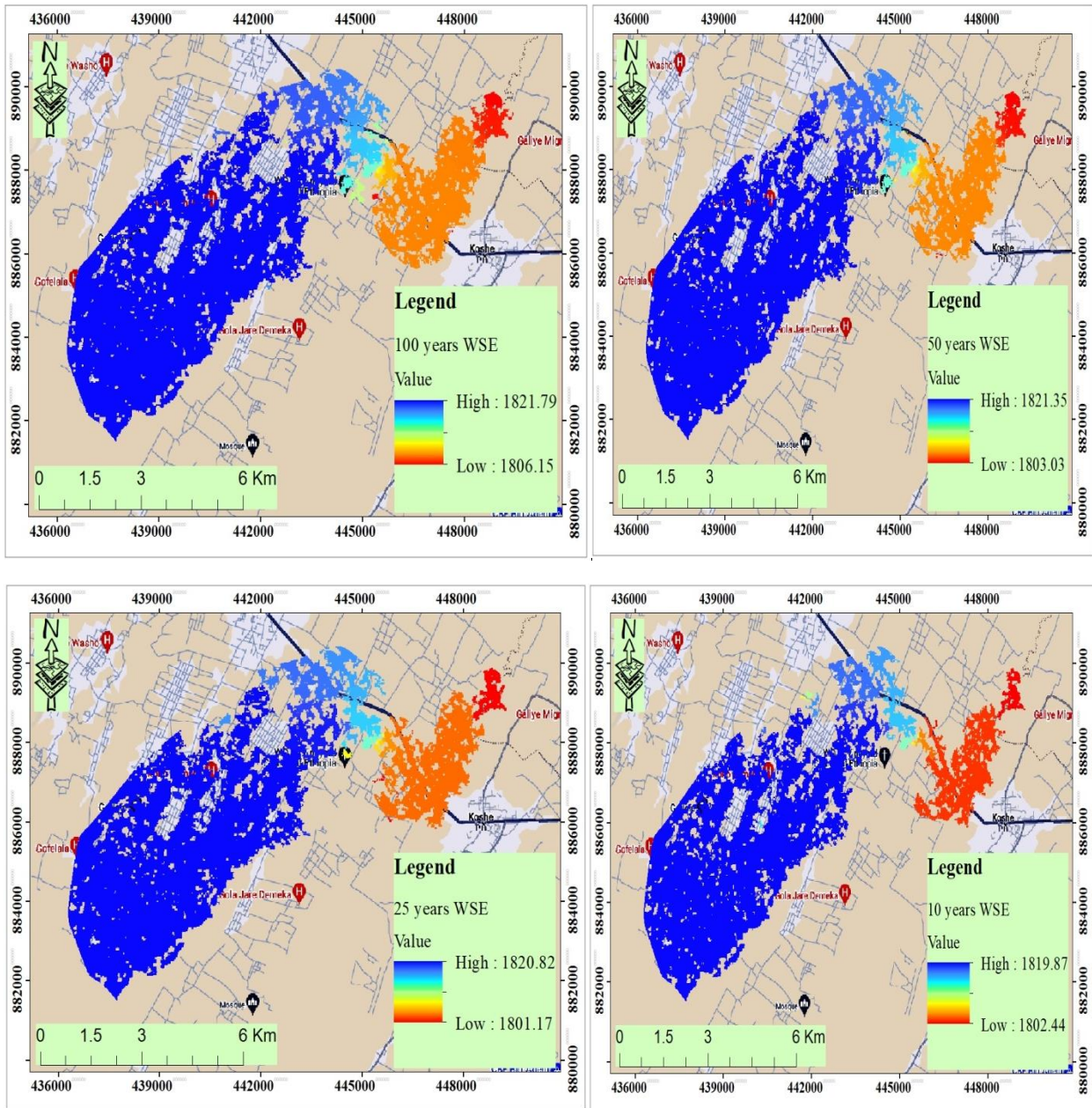
Appendix A: Maximum annual Rainfall

Year	Max ARF	Year	Max ARF
1992	44.7499	2007	54.1417
1993	57.6769	2008	61.4984
1994	68.9417	2009	73.6291
1995	69.6686	2010	47.5581
1996	68.0127	2011	47.5314
1997	61.7061	2012	33.5894
1998	65.0723	2013	45.3557
1999	57.4682	2014	34.4052
2000	52.1898	2015	27.406
2001	54.6545	2016	28.5207
2002	55.3332	2017	23.4149
2003	45.9506	2018	31.2065
2004	51.8322	2019	24.4825
2005	39.5311	2020	44.6989
2006	64.0965	2021	33.9369

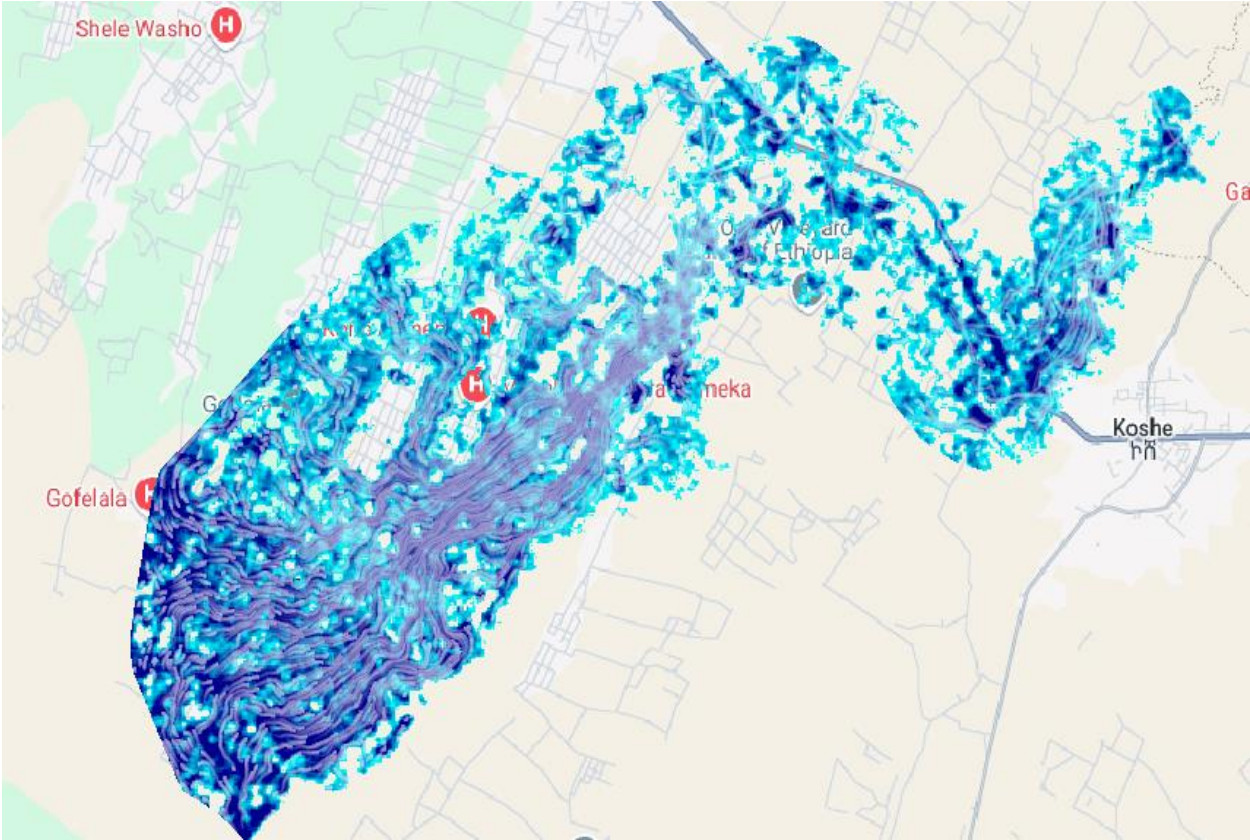
Appendix B: Flood inundation of Waja River floodplain



Appendix C: water surface elevation of Waja River floodplain



Appendix D: Particle tracing for 100 years flood



Appendix E: Field photos of flood inundated area at Goflala kebele





